AN ADVANCED LOAD FREQUENCY CONTROL BASED ON ADAPTIVE MODEL PREDICTIVE CONTROL

（適応モデル予測制御に基づく負荷周波数制御）

A Dissertation by

ADELHARD BENI REHIARA

Submitted in partial fulfillment of the requirement for the degree of Doctor of Engineering

Graduate School of Engineering
Department of System Cybernetics
Hiroshima University

March 2019

ACKNOWLEDGEMENT

I praise to the presence of God, because of His volition, I have completed my research and doctoral study at Electric Power and Energy System Laboratory (EPESL), System Cybernetics, Graduate School of Engineering, Hiroshima University.

First of all, I would like to address my acknowledgement to my supervisor, Professor Naoto Yorino, for professional support, excellent guidance, and patience, also for the opportunity to do the research at the Laboratory of EPES. Particularly, I would like to express my appreciation to all of EPESL member, especially to Professor Yoshifumi Zoka, Professor Yutaka Sasaki for giving me gracious support in my research as well as administrative support from Ms. Yukiko Yamauchi. I am also indebted to my committee member, Professor Katsuhiko Takahashi and Professor Ichiro Nishizaki, for their serving as board members.

My special thanks are expressed to my wife, Kastin, for her love, patience, and support in my life. Many thanks to my children, Lia, Willy and Kei, who made my stay in Japan more meaningful and enjoyable.

I am pleased to have the opportunity to meet Mr. Karar Al-Nagar, Mr. Muhammad Abdillah, Mr. Imam Wahyu, Mr. Ahmed Bedawy, Mr. Zulhaj Aliansyah and Mr. Samuel Mumbere who accompanied me during my study and my stay as well as Mr. Chong Kai, Mr. Hiroshi Zenitani, and Mr. Yuki Nakamura.

Finally, I would like to thanks to Mr. Edwin Tazelaar for the valuable discussion and comments and also to the financial support of the Indonesian Ministry of Research, Technology and Higher Education Directorate via General of Higher Education in the study and research

ABSTRACT

The growth of human population has increased the fossil fuel demand while the fuel reserves would not satisfy the demand in future. On the other hand, people have recognized that the use of fossil fuels has contributed to the increase in the temperature of the earth a few decades ago. Therefore the invention of the other energy sources are urgently needs as alternative energies. Renewable energy sources (RESs) from wind, solar, biomass, etc. seems to be the promising alternative energy since it is renewable by natural cycle and it is almost no pollution in converting and recycling. Unfortunately, RESs tend to be unstable and depend to the other variables such as weather, altitude, etc. Then the RESs penetration into power grid is not interested in the beginning of inventions.

Nowadays the researches and technology of RESs are almost mature and people have tried to send the energy to the power grid. Due to its unpredicted behavior, the stability and security of the power system will be the importance issues to be investigated. An Energy Management Systems (EMS) is introduced to face both stability and security problem due to the penetration of RESs into the power grid. This EMS system may include Load Frequency Control (LFC), Economic Dispatch, Unit Commitment, Load Forecasting, Interchange Schedule and Reserve Management into the system to find an optimal solution to distribute the energy while keeping the power system in stable.

An LFC system has played an importance role in an EMS system for maintaining load frequency in real time to ensure the frequency in stable condition and to keep the stability of power systems under load changes and fluctuation by maintaining power interchanges between areas. The penetration of RESs generation into power grid has introduced significant issues about power system stability and security. In such a way, the use of conventional controller may not sufficient to protect the power system against the power changes.

In this dissertation, an LFC in adaptive scheme is proposed to be applied in an EMS system. The adaptive controller adopts an internal model control (IMC) structures using two scenarios, i.e. static controller with adaptive internal model and both the adaptive controller and adaptive model. The adaptive feature is reaching by applying system identification method. Three area power system has been used to validate and to test the effectiveness of this controller through some case studies.

TABLE OF CONTENTS

LIST OF FIGURES

LIST OF TABLES

CHAPTER 1
INTRODUCTION

1.1 Background

An electric power system is one of the most complex dynamic systems and it consists of generation, transmission and distribution system and/or also loads as the user of the electrical power. The other electrical components that can probably be connected to the systems are transformer, circuit breaker, relay protection, prime mover, *etc*. which are used to supply, transmit and utilize electric power. All of the power system components are used to maintain the quality, continuity, stability and reliability of the systems [1]. Nowadays power system continues to expand in size and load demand; consequently, the maintenance of synchronism within the system has become increasingly difficult.

Load that connected to the power system can change every time. This condition will then influence frequency of the system. In the power system operation, deviation of frequency would be a critical issues since the deviation could cause many troubles to devices connected to the power system. It is reported that the frequency change will affect operation and speed control of both synchronous and asynchronous motors, increase reactive power consumption and furthermore degrade load performance,overload transmission lines and finally interfere system protection. Therefore a load frequency control is urgently needed to maintain the frequency stable during exchange power on the network where the generator dispatch must satisfy the load demand. Some works have been done in the area of load frequency control, including [2] designed an LFC using the model predictive control (MPC) for a multi-area power system including wind turbines, [3] presented a comparison of MPC and PI against a conventional Automatic Generation Control, [4] presented an LFC method based on Fuzzy Logic controller (FLC) and recently [5] discussed total tie line power flow by replacing the LFC model.

An energy management system (EMS) is a smart electrical network that incorporates advanced control and optimization strategies to reduce operation cost while keeping or even increasing the system reliability. The EMS system components can include: Load Frequency Control (LFC), Economic Dispatch, Unit Commitment, Load Forecasting, Interchange Schedule and Reserve Management. As a part of an EMS system, an LFC plays an importance rule to keep frequency in stable condition

and to keep the stability of power systems under load changes and fluctuation by maintaining power interchanges between areas. An EMS system includes many generators into the areas that introduce high non-linearity into the power grid. In addition, penetration of Renewable Energy generation into power grid has introduced significant issues about power system security. In such a way, the use of conventional controller may not sufficient to protect the power system against the power changes. The usage of smart controllers such as Neural Network, Fuzzy Control, and Model Predictive Control (MPC) are promisingly used to control the LFC but the degradation of controller performance can appear under the fluctuation of loads. Thus, an adaptive controller will be the solution to improve the controller performance while dealing with both non-linearity and power system security.

A Model Predictive Control (MPC) is an advanced control method that used a plant model to predict the optimal trajectory movement of the plant and the controller is used as the main controller of the proposed method. Then the main objective of this work is to develop an adaptive controller that can be applied to a Load Frequency Control (LFC). The adaptive controller adopts an internal model control (IMC) structures using two scenarios, i.e. static controller with adaptive internal model and both the adaptive controller and adaptive model. Results of the proposed method, including system identification are written in chapter 4.

Internal model is a process model that simulates the response of the system in order to estimate the outcome of a system disturbance. An Internal Model Control (IMC) can use the internal model to predict the future output of the plant and also to make correction of the output. This controller can be used to control a plant [6], to tune other controller [7], or to combine with the other controller such as PI/PID [7]–[12], Fuzzy controller [13], [14], Neural Network [15] or MPC [15]–[17].

1.2 Objective and Scope of the Study

Renewable energy sources (RESs) have been attracting human intention since the fossil fuel sources become vanished and currently the penetration of RESs into power grid is increasing together with the maturity of RESs technologies and researches. The RESs sources such as photovoltaic power generations (PVs) are expected to grow substantially in the near future. A reasonable estimation is that 20-30% of the amount of total energy will be delivered through such sources in the upcoming 10 years. PVs are clean energy sources, while they are prone to cause degradation of power quality as well as grid security due to unforeseen weather

conditions. Continuous sunlight intermittency, especially during cloudy days, incurs sudden intense changes in their outputs such as unpredictable significant ramp effect. The increasing renewable energy requires additional ramping abilities to maintain the grid stability. Development of sophisticated operation technology is a key subject [18].

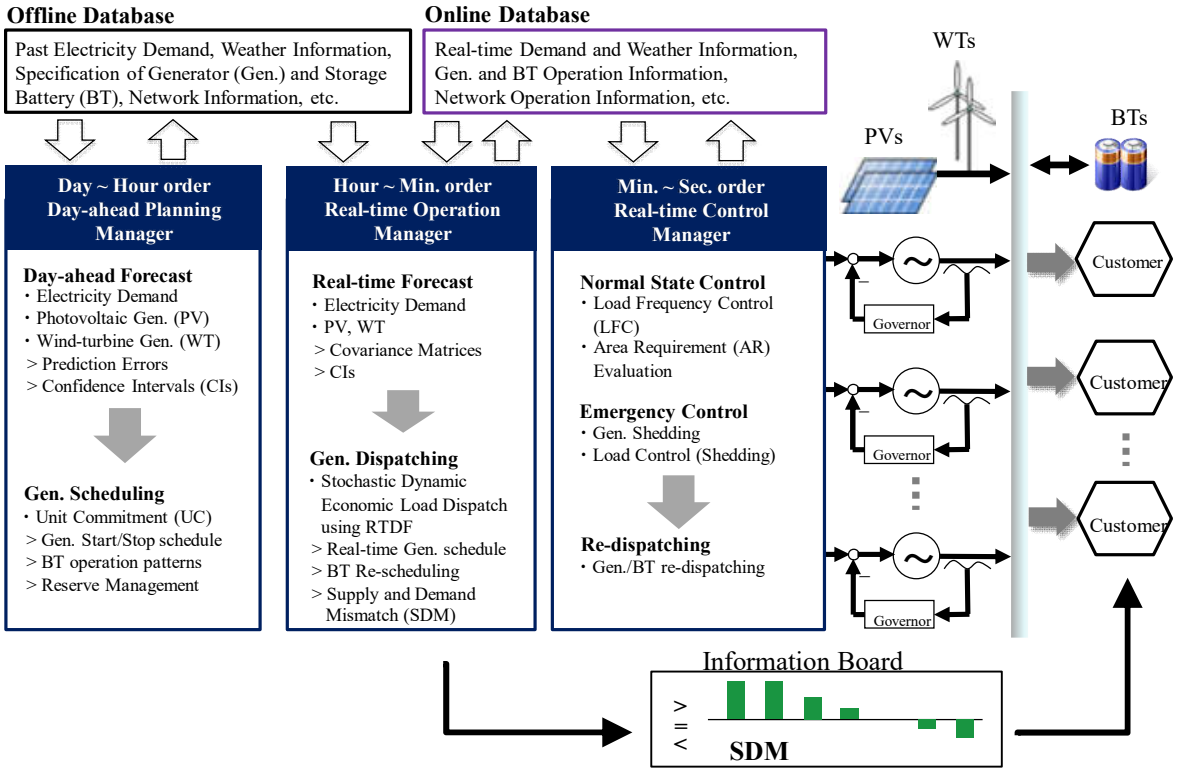

Fig. 1.1 Proposed EMS System

Our target is to develop a new EMS controller that enforces robustness against uncertainties [18]. Figure 1.1 shows the configuration of the proposed management system: there are mainly three functions responsible for day-ahead operation planning, minute-order real-time operation, and second-order real-time control. Based on the prediction of RES outputs, the system manages the existing generators, storage battery (BT) and controllable demands in optimal manner. We propose a new technique to be implemented in second-order manager.

a. Planning Manager

This manager provides an updated schedule of the output pattern for the limited resources. The output is represented as a 24-hour GS which also comprise the BT operation schedule, where a unit time is 30 minutes. Existing techniques for

the UC can be fully utilized in the optimization process. Uncertainties related to the prediction and fluctuation of PV are handled particularly [18][19].

b. Operation Manager

The operation manager provides real-time control signal to each generator based on most recent real-time forecast values. The optimization is performed in two stages. In stage I optimization, the 24-hour GS, which was planned in the previous day, is refined to determine the start/stop time schedule for generators. A robust GS against prediction error is determined. Stage II optimization utilizes only the start/stop time schedules and the BT operation. The rest of the optimization results of stage I is used only for reference and will be totally updated by the stage II optimization [18][19].

c. Control Manager

The uncertainty component can be dealt with the forecasting/planning department of the supply and demand control manager, but if prediction is lost, it must respond with excessive or insufficient power generation with real time control. The proposed method is related mainly to this part which is the main subject of this dissertation while the objective of this dissertation is to develop an adaptive controller that can be applied in an EMS system. The adaptive controller adopts an internal model control (IMC) structures using two scenarios, i.e static controller with adaptive internal model and both the adaptive controller and adaptive model[18][19].

1.3 Outline of the Thesis

The contents of the thesis are summarized as follows:

Chapter 1

This chapter presents the background of this research. The impact of power change and penetration of RESs into power grid to the power system stability and security. Then the proposed approach is outlined.

Chapter 2

In this chapter basic concept and definition of power system stability is described. It gives brief classification of power system stability. Modeling of synchronous generator is described in term of power system control.

Chapter 3

It describes the general concept of load frequency control. Effect of power changes and system responses are investigated. A case study is provided to express the effect of active power change and system frequency responses.

Chapter 4

The proposed method of a novel adaptive MPC controller to be applied in an LFC system is provided in this chapter. The adaptive feature is realized by using system identification method based on Prediction Error Minimization and Extreme Learning Machine method. It is shown that the proposed method has its advantages to overcome the incoming disturbance of the LFC system.

Chapter 5

As final conclussion, chapter 5 presents the resume of the major achievements. Furthermore, the future research works are provided to continue this research.

CHAPTER 2

POWER SYSTEM STABILITY AND GENERATION

2.1 Introduction

The Stability problem means to keep the synchronization and to return to normal operating conditions after disturbances in power system operation. The stability of the power system is a very important issue in supplying the energy to consumers. The stability problems which often happen are overload and inability of the system to provide the demand of reactive power. Both problems will bring the system to the condition of voltage collapse and frequency drop then finally blackout of the system. Voltage and frequency stability are usually happened in major disturbance which are including the increase in the load or very large power transfer. In this condition may cause the voltage in oscillation and the system will become instability.

The stability of the power system has become a major concern in an operating power system. The concern arises from the fact that in the steady-state conditions, the average speed for all generators should be the same. All disturbances in the power system will affect the synchronous operation i.e. suddenly changes of the load or loss of generated power can make significant influence of the system. The other type of disturbance is outage of transmission line(s), overload, or short circuit.

2.2 Classification of Power System Stability

There are three main concern in power system stability i.e. steady-state stability, transient stability, and dynamic stability[20].

Steady-state stability investigates power system ability to maintain stable under slow or gradual changes in power system operation. The steady-state stability study is usually done with load flow study to analyse of the power system capability including generators, transmission lines, transformers and other equipment to satisfy supplying the demand load. The power system phase angles should have not large changes and bus voltages should close to nominal values when demand load is applied.

Dynamic stability investigates power system ability to maintain stable under continuous small disturbance for longer time period, typically several minutes with the inclusion of control devices. It is done in small signal stability analysis to ensure that the variation in disturbance may not force the rotor angle to increase steadly.

Transient stability investigates power system ability to maintain stable under major disturbances. Following a disturbance, the power angle is change and then power system frequency undergo transient. The transient stability study is used to determine the power angle and synchronous machine frequency stability after sudden acceleration of the rotor shaft. Normally it is done in fist swing which is typically in one second after disturbance.

The disturbances in a power system could be faults, load changes, generator outages, line outages, voltage collapse or some combination of these [20]. Power system stability can be broadly classified into rotor angle, voltage and frequency stability as drawn in Fig. 2.1.

- ***Rotor Angle Stability***

The rotor angle of a generator depends on the balance between the electromagnetic torque due to the generator electrical power output and mechanical torque due to the input mechanical power through a prime mover. In case any changes of the system, the synchronism will be disturbed and the angle is introduced to be oscillated.

- ***Voltage Stability***

Voltage stability commonly happened in steady state condition, changes of the demand load can lead the steady state voltage to increase or decrease. The interested time frame of this stability can be 10 second to several minutes depending on the type of the disturbance. For long time changes of the load it can be treated as long term fault while for fast acting of devices, such as induction motors, power electronic drive, HVDC etc., it will be treated as short term fault.

- ***Frequency Stability***

Frequency stability refers to the ability of a power system to maintain steady frequency following a severe disturbance resulting large imbalance between generation and load. It depends on the ability to restore equilibrium between system generation and load, with minimum loss of load. Frequency instability may lead to sustained frequency swings leading to tripping of generating units or loads.

Power system stability is mainly concerned with the analysis of rotor stability. The stability classification into rotor angle, voltage and frequency stability is for simplifying analysis while those are influenced each other. Voltage alterations at a bus can influence rotor angle and frequency magnitude. Similarly, frequency drops can lead to the voltage collapse.

The main object to be analyzed in rotor angle stability and frequency stability is the power angle that depend on real power flow inside power grid. The large disturbance occurs, the large rotor angle being excursed so the rotor angle behavior should be discussed in transient stability. For small disturbance, the rotor angle is evaluated under linear assumption of the non-linearity representation.

The balanced power between generator and load will be the main focus of rotor angle stability and voltage stability. The rotor angle stability is focused on active power while reactive power is on voltage stability.

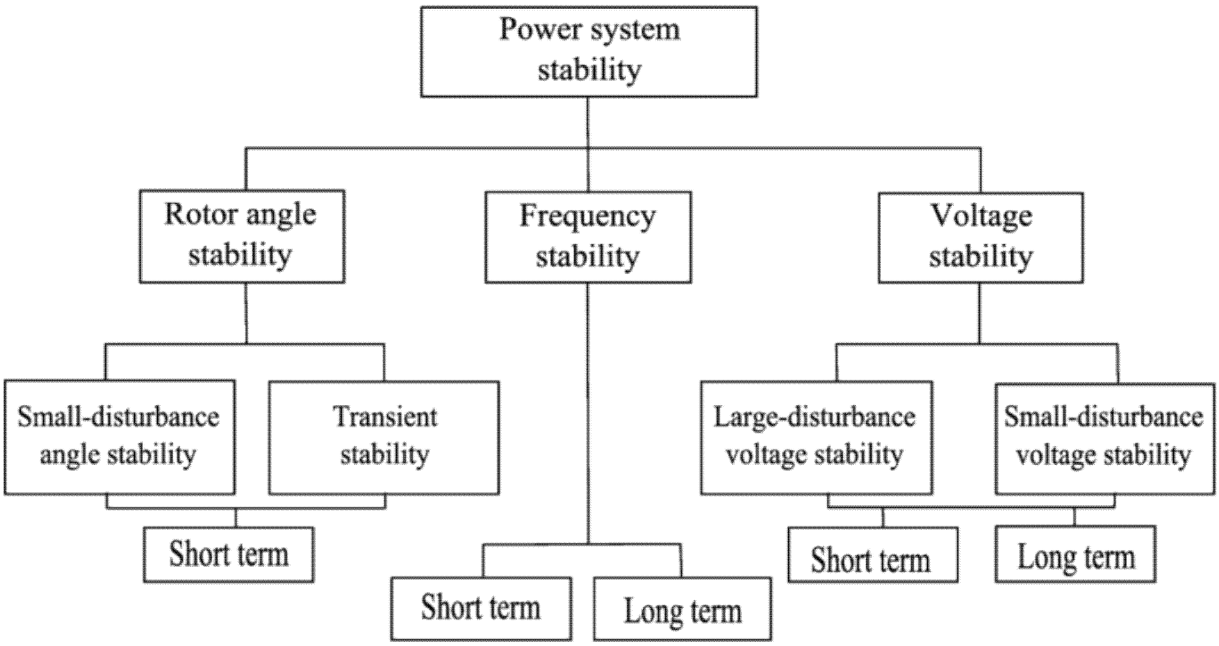

Fig. 2.1 Power system stability classification

2.3 Power System Control

Power Curve

As the main part of power system to provide and to absorb both active and reactive power, a synchronous generator is the main object in controlling power system. Therefore the active and reactive powers are controlled so that it meets the standard of frequency and voltage regulations while satisfying the power system reliability.

The generation of active and reactive power of a synchronous machine is related to the rated of the machine. The relationship between active and reactive generation is shown in Fig. 2.2 [20]. When the generator is overexcited, it will produce much reactive power then active power production is reduced while power

factor becomes smaller. On the other hand for under-excited generator, reactive power is absorbed from the grid while active power and power factor in same condition as overexcited generator.

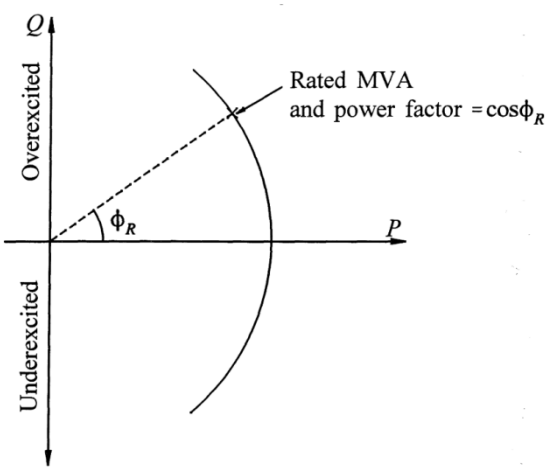

Fig. 2.2 Power generation of a generator

Swing Equation

Considering a synchronous alternator driven by a prime mover, the motion equation of the machine rotor is given by [20], [21].

$$J\frac{d^2\theta}{dt^2} = T_a = T_m - T_e \tag{2.1}$$

Where J, T_m, T_e and θ are the total moment of inertia of the rotor mass in kgm², mechanical torque supplied by the prime mover in N-m, the electrical torque output of the alternator in N-m and the angular position of the rotor in rad respectively.

In the steady state, the electrical torque is equal to the mechanical torque, and hence by neglecting the losses the accelerating torque T_a will be zero. During this period the rotor will move at synchronous speed ω_s in rad/s.

The angular position θ is measured with a stationary reference frame. To represent it with respect to the synchronously rotating frame, we define [20], [21].

$$\theta = \omega s + \delta \tag{2.2}$$

Where δ is the angular position in rad with respect to the synchronously rotating reference frame. Taking the time derivative of the above equation we get

$$\omega_r = \frac{d\theta}{dt} = \omega_S + \frac{d\delta}{dt} \tag{2.3}$$

Defining the angular speed of the rotor as in equation (2.3) can be simplifying as follows [20], [21]:

$$\omega_r - \omega_S = \frac{d\delta}{dt} \tag{2.4}$$

The error in speed is expressed as $^{d\delta}/_{dt}$ since it is clearly stated in eq. (2.4) that the rotor angular speed is equal to the synchronous speed only when $^{d\delta}/_{dt}$ is equal to zero. If there is acceleration in rotor angular speed, eq. (2.3) will become [20], [21]:

$$\frac{d^2\theta}{dt^2} = \frac{d^2\delta}{dt^2} \tag{2.5}$$

Substitute equation (2.5) to equation (2.1) and expressed as in equation (2.6). Equation (2.7) expresses equation (2.6) in terms of power by multiplying both sides with ω_r [20], [21].

$$J\frac{d^2\delta}{dt^2} = T_a = T_m - T_e \tag{2.6}$$

$$J\omega_r\frac{d^2\delta}{dt^2} = \omega_r T_m - \omega_r T_e = P_m - P_e \tag{2.7}$$

Where P_m and P_e are the mechanical and electrical in MW respectively. Inertia constant H is described as stored kinetic energy at synchronous speed (Mega Joule) divided by the generator MVA based. In terms of inertia constant H, eq. (2.7) can be normalized as follows [20], [21].

$$2H\frac{S_{rated}}{\omega_s^2}\omega_r\frac{d^2\delta}{dt^2} = P_m - P_e \tag{2.8}$$

$$H = \frac{J\omega_s^2}{2S_{rated}} \tag{2.9}$$

In steady state, the machine angular speed is equal to the synchronous speed and hence ω_r is replaced by ω_s. Equation (2.10) expressed these quantities in per unit by dividing both sides of (2.8) by S_{rated} [20], [21].

$$\frac{2H}{\omega_s}\frac{d^2\delta}{dt^2} = P_m - P_e \quad \text{per unit} \tag{2.10}$$

Equation (2.10) describes the behavior of the rotor dynamics and hence is known as the swing equation. The angle δ is the angle of the internal EMF of the

generator and it dictates the amount of power that can be transferred. This angle is therefore called the load angle.

Typical Value of H

While H is called inertia constant, it seems to be changed together with the deviation of rotor speed from the synchronous speed. However since ω_r does not have much change before losing the stability, H is evaluated at the synchronous speed and so it is considered to remain constant.

Table 2.1 provides typical value of inertia constant of thermal and hydraulic generating units which represents the combined inertia of the generator and the turbine [20].

Table 2.1 Typical H value

Type of generating unit	H
Thermal unit	
• 3600 rpm (2 poles)	2.5 - 6.0
• 1800 rpm (4 poles)	4.0 - 10.0
Hydraulic unit	2.0 - 4.0

2.3.1 Dynamic Model of Synchronous Generator

A simplified frequency response model for a single area power system with generator–load dynamic relationship between the incremental mismatch power ($\Delta P_m - \Delta P_L$) and the frequency deviation (Δf) can be expressed as [2]:

$$s\Delta f = \left(\frac{1}{2H}\right)\Delta P_m - \left(\frac{1}{2H}\right)\Delta P_L - \left(\frac{D}{2H}\right)\Delta f \tag{2.11}$$

The dynamic of the governor can be expressed as:

$$s\Delta P_m = \left(\frac{1}{T_t}\right)\Delta P_g - \left(\frac{1}{T_t}\right)\Delta P_m \tag{2.12}$$

The dynamic of the turbine can be expressed as

$$s\Delta P_g = \left(\frac{1}{T_g}\right)\Delta P_c - \left(\frac{1}{RT_g}\right)\Delta f - \left(\frac{1}{T_g}\right)\Delta P_g \tag{2.13}$$

Equations 2.11-2.13 represent a simplified frequency response model for one generator unit and can be combined in the following state space model as:

$$\begin{bmatrix} s\Delta P_g \\ s\Delta P_m \\ s\Delta f \end{bmatrix} = \begin{bmatrix} -\frac{1}{T_g} & 0 & -\frac{1}{RT_g} \\ \frac{1}{T_t} & -\frac{1}{T_t} & 0 \\ 0 & \frac{1}{2H} & -\frac{D}{2H} \end{bmatrix} \begin{bmatrix} \Delta P_g \\ \Delta P_m \\ \Delta f \end{bmatrix} + \begin{bmatrix} -\frac{1}{2H} & 0 \\ 0 & -\frac{1}{T_g} \\ 0 & 0 \end{bmatrix} \begin{bmatrix} \Delta P_L \\ \Delta P_c \end{bmatrix} \quad 2.14$$

Where ΔP_g, ΔP_m, Δf, ΔP_L, ΔP_c, y, H, D, R, T_g and T_t are the governor output change, the mechanical power change, the frequency deviation, the load change, supplementary control action, system output, equivalent inertia constant, equivalent damping coefficient, speed droop characteristic, governor time constants, and turbine time constants respectively.

2.3.2 Excitation System of Synchronous Generator

Excitation system models in the meaning of structure and implemented controller type are classified and standardized. There are nineteen different excitation types in three major groups: Direct Current Commutate Exciters (type DC), Alternator Supplied Rectifier Excitation Systems (type AC) and Static Excitation Systems (type ST) [20]. All these models include linear controllers because they are mostly used in practice. Linear regulation is good for stationary state, but in transition state quality of regulation changes with change of operating point which introduces a nonlinear system for synchronous generator.

Power transmitted between the two machines is proportional to the internal voltages (E and E') of the two machines, divided by the reactance. The power will be increased if either internal voltage is increased (Eq. 2.15). Therefore, it is apparent that raising the internal voltage increases the stability limits.

In the transient condition when the fault occurs, during the fault the flux linkage decays by the short circuit time constant. If the fault is maintained for a long time the machine might survive the first swing of its rotor, but because of the continued decrease in filed flux linkage it might pull out of step in the second swing or the next one. A controlled excitation system can control the flux linkage in order to prevent the loss of synchronism. Hence the excitation system can assist transient stability even though high-speed clearing of fault is applied. The faster the excitation system responds to correct low voltage, the more effective improvement will be achieved in stability [20].

In the per unit system, because the rotor speed is equal to one due to synchronize speed, the power P is equivalent to the electrical torque, and they are both provided by the classical power transfer equation [22]:

$$T_e = P = \left(\frac{E' E_s}{X_T} \right) \sin \delta_0 \tag{2.15}$$

Because the electrical torque variation (T_e) in eq. (2.15) is proportional to the variation of the generator internal angle δ, this electrical torque type is called the synchronous torque. A small increment of the electrical torque around the quiescent point of operation can be expressed as [22]:

$$\Delta T_{sync} = K_1 \Delta \delta \tag{2.16}$$

Where $K_1 = \left(\frac{E' E_s}{X_T} \right) \cos \delta_0$

Another electrical torque exists in a machine that is proportional to the speed variation of the machine. This electrical torque is called the damping torque (T_{damp}) and so electric torque can be rewritten as [22]:

$$\Delta T_e = \Delta T_{sync} + \Delta T_{damp} = K_1 \Delta \delta + K_D \Delta \omega \tag{2.17}$$

The dynamic equation of the machine rotor corresponds to the acceleration law of the rotating bodies and can be expressed as [22]:

$$s\Delta\omega = \frac{1}{M} \left(\Delta T_{sm} - \Delta T_{sync} - \Delta T_{damp} \right) \tag{2.18}$$

$$s\Delta\delta = \omega_0 \Delta\omega \tag{2.19}$$

Therefore the simplified excitation model in a synchronous generator can be expressed in state space system as [22]:

$$\begin{bmatrix} s\Delta\delta \\ s\Delta\omega \end{bmatrix} = \begin{bmatrix} 0 & \omega_0 \\ -\frac{K_1}{M} & -\frac{K_D}{M} \end{bmatrix} \begin{bmatrix} \Delta\delta \\ \Delta\omega \end{bmatrix} + \begin{bmatrix} 0 \\ \frac{1}{M} \end{bmatrix} \Delta T_m \tag{2.20}$$

$$y = \begin{bmatrix} 1 & 0 \end{bmatrix} \begin{bmatrix} \Delta\delta \\ \Delta\omega \end{bmatrix} \tag{2.21}$$

Where *Tm, H, M,* K_1 and K_D are mechanical power input variation (pu), inertia constant (sec.), inertia coefficient = 2*H* (sec), base rotor electrical speed (377 rad/s), rotor angle (rad), synchronous constant, and damping constant respectively.

The response of a generator voltage when subjected to major disturbances is highly influence by the excitation control system [23].

2.3.3 Active Power Control

Active power in a power system is mainly controlled trough generator which is mostly synchronous generator. For an isolated power system, power interchange is no need to be maintenance and so an Automatic Generator Control (AGC) can handle the active power in to the system. On the other hand for large power system with many areas where the power interchange is an importance issue, a Load Frequency Control is needed to maintain the frequency.

Single line diagram for a synchronous machine with transient reactance X_s and armature voltage E connected to an infinite bus through reactance X_e of the line and terminal voltage V as shown in Fig. 2.3. The power flow obtained from the figure is formulated as follows [20], [21].

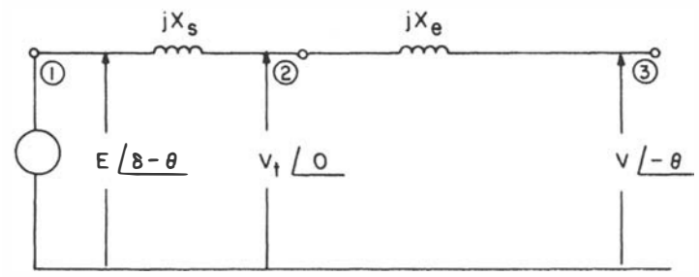

Fig. 2.3 A synchronous machine connected to infinity bus

$$P = \frac{EV_t \sin(\delta - \theta)}{X_s} \tag{2.22}$$

$$Q = \frac{EV_t \cos(\delta - \theta) - V_t^2}{X_s} \tag{2.23}$$

By assuming that there is power loss, active power P can be reformulate based on power transfer from node 1 to 3 across total reactance X_t and from node 2 to 3 across line reactance X_e as in 3. Based on this equation, the armature voltage E can be obtained as in eq. (2.25) [20], [21].

$$P = \frac{EV \sin\delta}{X_t} = \frac{V_t V \sin\theta}{X_e} \tag{2.24}$$

$$E = V_t \frac{X_t \sin\theta}{X_e \sin\delta} \tag{2.25}$$

Equation (2.26) and (2.27) in then formulated by substituting (2.25) to (2.22) and (2.23) [20], [21].

$$P = \frac{V_t^2 X_t}{X_s X_e \sin\delta}\left[\sin\theta \sin(\delta-\theta)\right] \tag{2.26}$$

$$Q + \frac{V_t^2}{X_s} = \frac{V_t^2 X_t}{X_s X_e \sin\delta}\left[\sin\theta \cos(\delta-\theta)\right] \tag{2.27}$$

Since {sinα sinβ=½[cos(α-β)-cos(α+β)]} and {sinα cosβ=½[sin(α+β)+sin(α-β)]}, (2.26) and (2.27) can be rearranging as in (2.28) and (2.29)[20], [21].

$$P + \frac{V_t^2 X_t}{2X_s X_e \tan\delta} = \frac{V_t^2 X_t}{2X_s X_e \tan\delta}\cos(\delta - 2\theta) \tag{2.28}$$

$$Q - \frac{V_t^2 (X_s - X_e)}{2X_s X_e} = \frac{-V_t^2 X_t}{2X_s X_e \sin\delta}\sin(\delta - 2\theta) \tag{2.29}$$

By adding (2.28) and (2.29) and taking square for both sides, a new equation is formulated.

$$\left[P + \frac{V_t^2 X_t}{2X_s X_e \tan\delta}\right]^2 + \left[Q - \frac{V_t^2 (X_s - X_e)}{2X_s X_e}\right]^2 = \left[\frac{V_t^2 X_t}{2X_s X_e \sin\delta}\right]^2 \tag{2.30}$$

It is noted from eq. (2.30) that by setting power angle δ, active power P can be adjusted and reactive power Q will follow the setting under circle bound within radius R as shown in (2.31)-(2.33)[20], [21].

$$P_0 = \frac{-V_t^2 X_t}{2X_s X_e \tan\delta} \tag{2.31}$$

$$Q_0 = \frac{V_t^2}{2}\left(\frac{1}{X_e} - \frac{1}{X_s}\right) \tag{2.32}$$

$$R_0 = \frac{V_t^2}{2\sin\delta}\left(\frac{1}{X_s} + \frac{1}{X_e}\right) \tag{2.33}$$

On the other hand the static limit of the curve is obtained by setting power angle δ to 90° as shown in (2.34). This static limit will determine the minimum permissible output VAR for generated watts at the voltage terminal specifications. The stability limit can be figured in Fig. 2.4[20], [21].

$$P^2 + \left[Q - \frac{V_t^2}{2}\left(\frac{1}{X_e} - \frac{1}{X_s}\right)\right]^2 = \left[\frac{V_t^2}{2}\left(\frac{1}{X_s} + \frac{1}{X_e}\right)\right]^2 \tag{2.34}$$

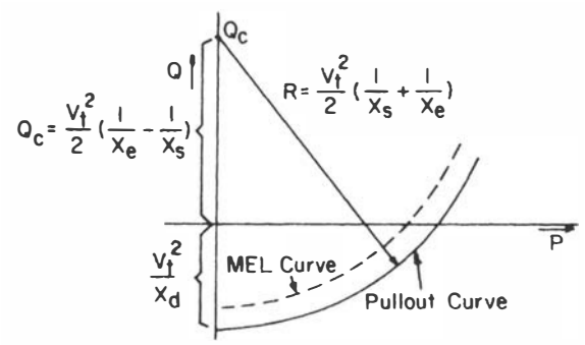

Fig. 2.4 Static stability limit of a synchronous machine

2.4 Summary

This section introduce general concept of power system stability and control. The basic concept of power system stability is described in the beginning of this chapter. In terms of power system control, dynamic of synchronous generator and excitation model and also the basic of active power control as the part of frequency control are introduced.

CHAPTER 3
LOAD FREQUENCY CONTROL

3.1 Introduction

In the power system operation, deviation of frequency would be a critical issues since the deviation could cause many troubles to devices connected to the power system. It is reported that the frequency change will affect operation and speed control of both synchronous and asynchronous motors, increase reactive power consumption and furthermore degrade load performance,overload transmission lines, and finally interfere system protection. Nowadays, the complexity of power system stability is increasing due to rapid increase in renewables such as solar generations [24].

However, nowadays frequency stability is a major issue in power system operation due to continuous output change of renewables such as wind and solar generations. The complexity is increasing in the operation of multi-area power system, where the system characteristics may vary depending on system conditions. Therefore, a Load Frequency Control (LFC) is required to respond faster and to improve frequency stability [25].

Load frequency control (LFC) is one of the main parts on power system to maintain the frequency fluctuation of load change. The main function of LFC is to maintain the frequency stable during exchange power by minimizing frequency deviation on the network where the generator dispatch mustsatisfy the load demand [25]–[28].

3.2 Power System Model

Power system model is described using a differential algebraic equation (DAE) as [3], [26], [27]:

$$\dot{x} = f(x,q,u,w) \tag{3.1}$$

$$0 = g(x,q,u,w) \tag{3.2}$$

Where x, q, u and w are the dynamic system states, the algebraic system states, the controller inputs and the system disturbance respectively. The algebraic states are not appeared in DAE so that it can be removed from the (3.1) and (3.2). The (3.1)

is called differential variable and (3.2) is an algebraic equation or well known as a constraint.

Mathematical Modelling of Generator

Applying the swing equation of a synchronous machine to small perturbation, we have [20][21]:

$$\frac{2H}{\omega}\frac{d^2\Delta\delta}{dt^2} = \Delta P_m - \Delta P_e \tag{3.3}$$

Or in terms of small deviation in speed (3.4) and its Laplace transform in (3.5).

$$\frac{d\Delta\frac{\omega}{\omega_s}}{dt} = \frac{1}{2H}(\Delta P_m - \Delta P_e) \tag{3.4}$$

$$\Delta\Omega(s) = \frac{1}{2Hs}(\Delta P_m(s) - \Delta P_e(s)) \tag{3.5}$$

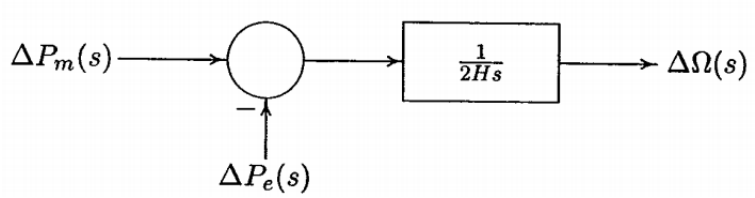

Fig. 3.1 Block diagram for generator

Mathematical Modelling of Load

The load on the power system consists of a variety of electrical drives. The equipment used for lighting purposes are basically resistive in nature and the rotating devices are basically a composite of the resistive and inductive components. The speed-load characteristic of the composite load is given by [20][21]:

$$\Delta P_e = \Delta P_L + D\Delta\omega \tag{3.6}$$

Where ΔP_L is the non-frequency- sensitive load change, $D\Delta\omega$ is the frequency sensitive load change. D is expressed as percent change in load by percent change in frequency.

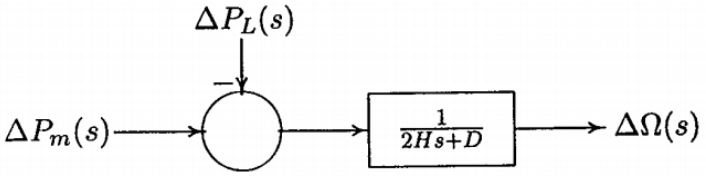

Fig. 3.2 Generator and Load block diagram

Mathematical Modelling for Prime Mover

The source of power generation is commonly known as the prime mover. It may be hydraulic turbines at waterfalls, steam turbines whose energy comes from burning of the coal, gas and other fuels. The model for the turbine relates the changes in mechanical power output ΔP_m to the changes in the steam valve position ΔP_V[20][21].

$$G_T = \frac{\Delta P_m(s)}{\Delta P_V(s)} = \frac{1}{1+\tau_T s} \tag{3.7}$$

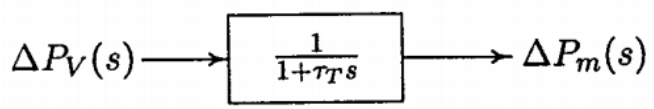

Fig. 3.3 Block diagram for prime mover

Where τ_T is the turbine constant which has the range in between 0.2 and 2.0 seconds.

Mathematical Modelling for Governor

When the electrical load is suddenly increased then the electrical power exceeds the mechanical power input. As a result of this the deficiency of power in the load side is extracted from the rotating energy of the turbine. Due to this reason the kinetic energy of the turbine i.e. the energy stored in the machine is reduced and the governor sends a signal to supply more volumes of water or steam or gas to increase the speed of the prime-mover so as to compensate speed deficiency.

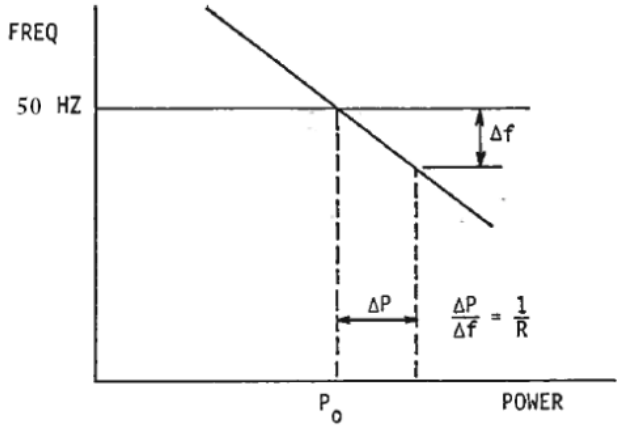

Fig. 3.4 Graphical Representation of speed regulation by governor

The slope of the curve represents speed regulation *R*. Governors typically have a speed regulation of 5-6 % from no load to full load [20][21].

$$\Delta P_g = \Delta P_{ref} - \frac{1}{R}\Delta f \tag{3.8}$$

The command ΔP_g is transformed through hydraulic amplifier to the steam valve position command ΔP_V. We assume a linear relationship and consider simple time constant τ_g we have the following s-domain relation [20][21]:

$$\Delta P_V(s) = \frac{1}{1+\tau_g}\Delta P_g(s) \tag{3.9}$$

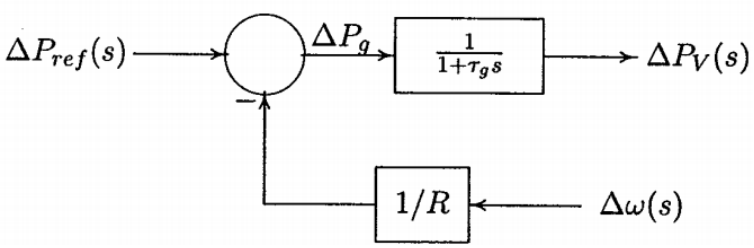

Fig. 3.5 Block diagram for governoor

Combining all the block diagrams from earlier block diagrams for a single are system we get the following [20][21]:

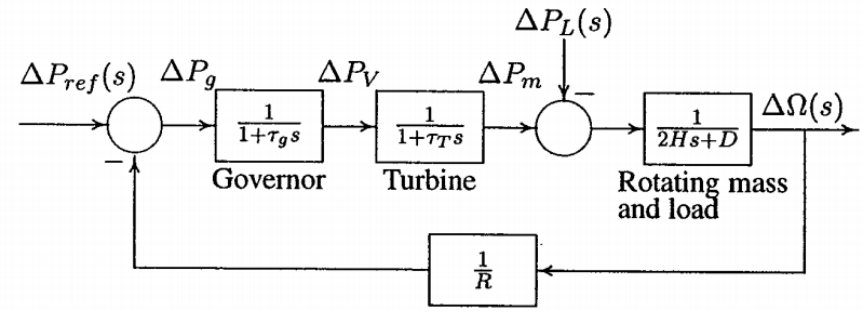

Fig. 3.6 Completed power system block diagram

A completed LFC block diagram including controller and tie line power change can be redrawn in Fig. 3.7 [24]–[27], [29].

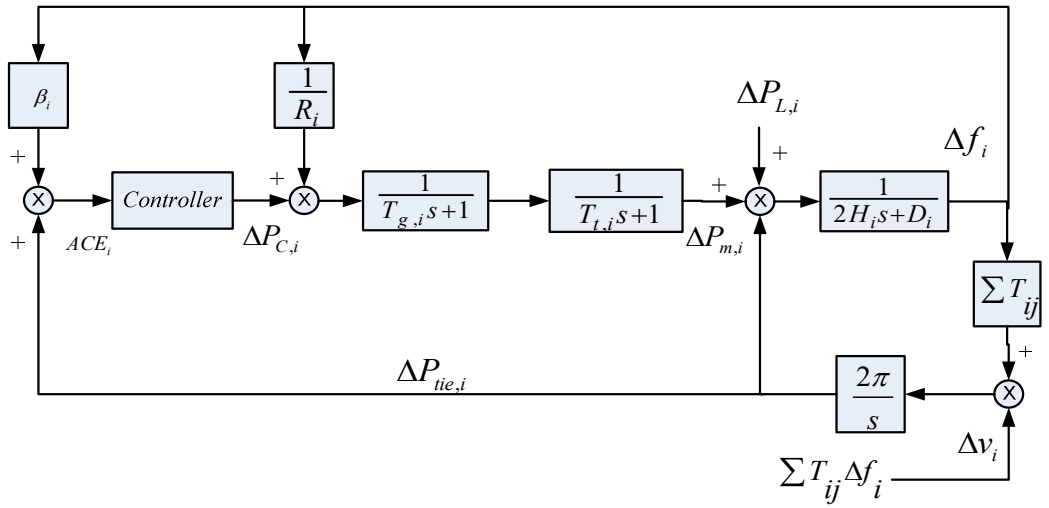

Fig. 3.7 Power system dynamics

The tie-line power change P_{tie} is calculated for all area n using (3.10) and the area control error (ACE) which is a suitable linear combination of frequency f and tie-line power changes for each area is found using (3.11) as follows [2], [26], [27].

$$\Delta P_{tie,i} = \frac{2\pi}{s}\left[\sum_{\substack{j=1 \\ j\neq i}}^{n} T_{ij}\Delta f_i - \sum_{\substack{j=1 \\ j\neq i}}^{n} T_{ij}\Delta f_j\right] \tag{3.10}$$

$$ACE_i = \Delta P_{tie,i} + \beta_i \Delta f_i \tag{3.11}$$

State space model for this power system model can be described in following equation.

$$\dot{x}(t) = Ax(t) + Bu(t) + Fw(t) \tag{3.12}$$

$$y(t) = Cx(t) + Du(t) \tag{3.13}$$

where

$x(t)$ = State variables = $[\Delta P_{g,i}\ \Delta P_{m,i}\ \Delta f_i\ \Delta P_{tie,i}]^T$

$u(t)$ = Input variables = $[\Delta P_{L,i}\ \Delta v_{,i}]^T$

$w(t)$ = Control variable = $\Delta P_{c,i}$

$y(t)$ = Output variable = ACE_i

The feed forward matrix of the can be removed from the system matrices model since there is no direct connection between input and output variable. Therefore all of the matrices of the system model can be written in (3.14)-(3.17) [2], [26], [27].

$$A_i = \begin{bmatrix} -\frac{1}{T_{g,i}} & 0 & -\frac{1}{R_i T_{g,i}} & 0 \\ \frac{1}{T_{t,i}} & -\frac{1}{T_{t,i}} & 0 & 0 \\ 0 & \frac{1}{2H_i} & -\frac{D_i}{2H_i} & -\frac{1}{2H_i} \\ 0 & 0 & 2\pi\sum_{\substack{j=1 \\ j\neq i}}^{N} T_{ij} & 0 \end{bmatrix} \tag{3.14}$$

$$B_i = \begin{bmatrix} \frac{1}{T_{g,i}} & 0 & 0 & 0 \end{bmatrix}^T \tag{3.15}$$

$$C_i = \begin{bmatrix} 0 & 0 & \beta_i & 1 \end{bmatrix} \tag{3.16}$$

$$F_i = \begin{bmatrix} 0 & 0 \\ 0 & 0 \\ -\frac{1}{2H_i} & 0 \\ 0 & -2\pi \end{bmatrix} \tag{3.17}$$

Where $P_{g,i}$ is the governor output, $P_{m,i}$ is the mechanical power, $P_{L,i}$ is the load/disturbance, $P_{c,i}$ is the control action, y_i is the system output, H_i is the equivalent inertia constant, d_i is the equivalent damping coefficient, R_i is the speed droop characteristic and β_i is the a frequency bias factor of area i. T_{ij} is the tie-line synchronizing coefficient with area j, $T_{g,i}$ and $T_{t,i}$ are the governor and turbine time constants of area i.

3.3 Effect of the Active Power Change

Power systems are tends to become larger in size since the demand load is increasing by the time. Normally generator and load are separated in distance and so it is need to be grouped into areas. To maintain power flow between areas, a load frequency control can represent whole areas in terms of control area. For an isolated power system, power interchange is no need to be maintenance and so an Automatic Generator Control (AGC) can handle the active power in to the system. On the other hand for large power system with many areas where the power interchange is an importance issue, a Load Frequency Control is needed to maintain the frequency. Fig. 1 shows a two areas power system, which is used to investigate power control in a power system [20].

In a steady state condition, the frequency for both areas is same; therefore frequency deviation is zero and total load change is shown in (3.18).

$$\Delta f = \Delta\omega_1 = \Delta\omega_2 = \frac{-\Delta P_L}{\left(1/R_1 + 1/R_2\right)\left(D_1 + D_2\right)} \tag{3.18}$$

If there is any change in area 1, this equation becomes (3.19) which is spreaded into the frequency change equation in area 1 and 2 as shown in (3.20) and (3.21).

$$\Delta f = \frac{-\Delta P_{12} - \Delta P_{L1} + \Delta P_{21}}{\left(1/R_1 + 1/R_2\right)\left(D_1 + D_2\right)} \tag{3.19}$$

$$\Delta f\left(1/R_1+D_1\right)=-\Delta P_{12}-\Delta P_{L1} \tag{3.20}$$

$$\Delta f\left(1/R_2+D_2\right)=\Delta P_{21} \tag{3.21}$$

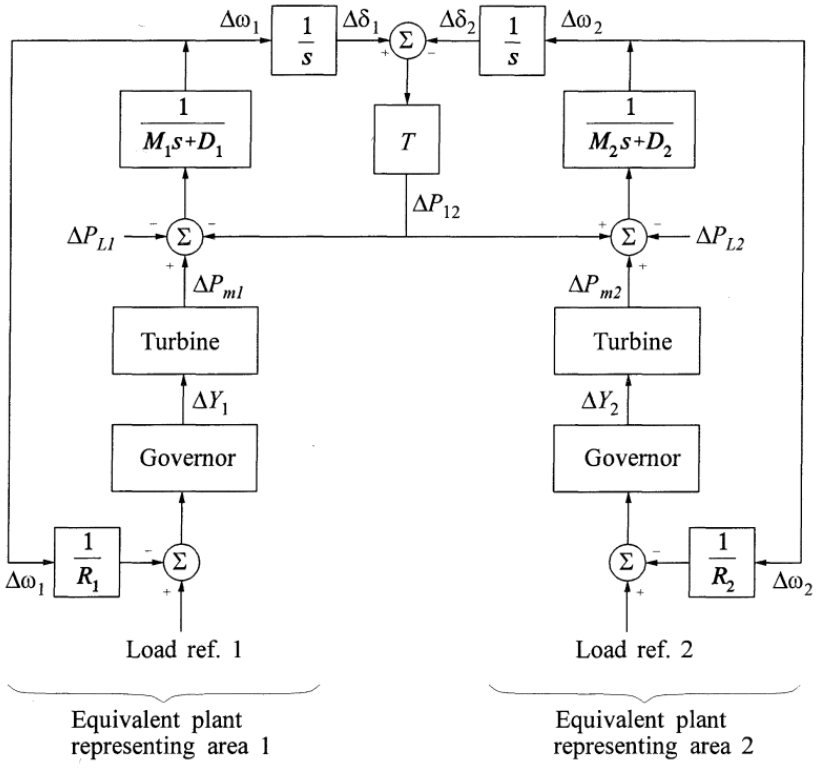

Fig. 3.8 Two Area power system

Equation (3.22) and (3.23) are done by substituting (3.21) into (3.20) and (3.20) into (3.21) respectively. Where β_1 and β_2 are denoted as frequency bias in area 1 and 2.

$$\Delta f=\frac{-\Delta P_{L1}}{\left(1/R_1+D_1\right)+\left(1/R_2+D_2\right)}=\frac{-\Delta P_{L1}}{\beta_1+\beta_2} \tag{3.22}$$

$$\Delta P_{12}=\frac{-\Delta P_{L1}\left(1/R_2+D_2\right)}{\left(1/R_1+D_1\right)+\left(1/R_2+D_2\right)}=\frac{-\Delta P_{L1}\beta_2}{\beta_1+\beta_2} \tag{3.23}$$

It is seen from (3.22) and (3.23) that the change in ΔP_{L1} will reduce frequency in both area and introduce a tie line flow ΔP_{12}. Positive sign of ΔP_{12} in area 2 means that area 2 will send power to area 1. In same way if the change is come from area 2, the frequency and tie line power is expressed in (3.24) and (3.25).

$$\Delta f = \frac{-\Delta P_{L2}}{\beta_1 + \beta_2} \tag{3.24}$$

$$\Delta P_{12} = -\Delta P_{21} = \frac{\Delta P_{L2}\beta_1}{\beta_1 + \beta_2} \tag{3.25}$$

3.4 System Response of Power Change

Consider a single machine system connected to an infinite bus as shown in Fig. 3.9, its swing equation in steady state condition can be expressed as follows [20].

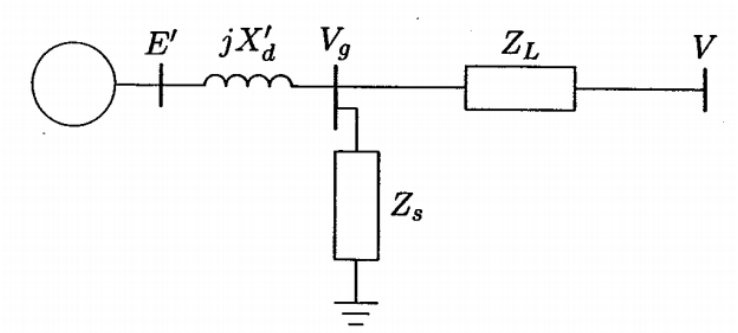

Fig. 3.9 Single machine system

$$\frac{H}{\pi f_0}\frac{d^2\delta}{dt^2} = \Delta P_m - \Delta P_{\max}\sin\delta \tag{3.26}$$

If there is some change in mechanical power input P_m as the result of disturbances or load changes, power angle δ will change to a new state as $\delta=\delta_0+\Delta\delta$. Then it will further influence swing equation into (3.27). The change affects the swing equation in terms of incremental changes in power angle as in (3.28).

$$\frac{H}{\pi f_0}\frac{d^2\delta_0}{dt^2} + \frac{H}{\pi f_0}\frac{d^2\Delta\delta}{dt^2} = \Delta P_m - \Delta P_{\max}\sin\delta_0 - \Delta P_{\max}\cos\delta_0\Delta\delta \tag{3.27}$$

$$\frac{H}{\pi f_0}\frac{d^2\Delta\delta}{dt^2} + \Delta P_{\max}\cos\delta_0\Delta\delta = 0 \tag{3.28}$$

The quantity of $P_{max}\cos\delta_0$ is known as synchronizing coefficient P_s which is the slope of power angle curve at δ_0. The root(s) of the second order differential equation in (3.28) can be shown in (3.29).

$$s^2 = -\frac{\pi f_0}{H}P_S \tag{3.29}$$

It can be seen from (3.29) that if P_s is negative, there is a root in the right-half s-plane and so the system will be unstable and the response will increase

exponentially. On the other hand, while P_s is positive, two roots will appear in j-ω axis and the response is oscillatory and undamped. The system is stable with a natural frequency oscillation as given in (3.30).

$$\omega_n = \sqrt{\frac{\pi f_0}{H} P_S} \tag{3.30}$$

3.5 Case Studies

The effect of power change is simulated in this case that also compare the controller performance of PI and MPC controller used in this simulation. The configuration of investigated multi-area power system is depicted in Fig. 3.10. The power system configuration is based on [2], [24]–[27], [30], with its parameter as shown in Table 3.1 while the system dynamics is figured in Fig. 3.7.

An investigation without controller action is done by applying 0.6 pu disturbance for all area in about 30s and the result is shown in Fig. 3.11. It seems that frequency deviation (Δf) in all areas is going to decay in the point of 1.6 Hz so that the frequency will become lower than its standard without controller. By the way prime mover P_m in all area should supply the demand power to be injected to the system. The system will need any controller to drive the frequency back by occupying some generators in the system. The rank of each area's state matrix is 4 as same with its dimension. Therefore the system can be fully controllable. This case studies are based on [26].

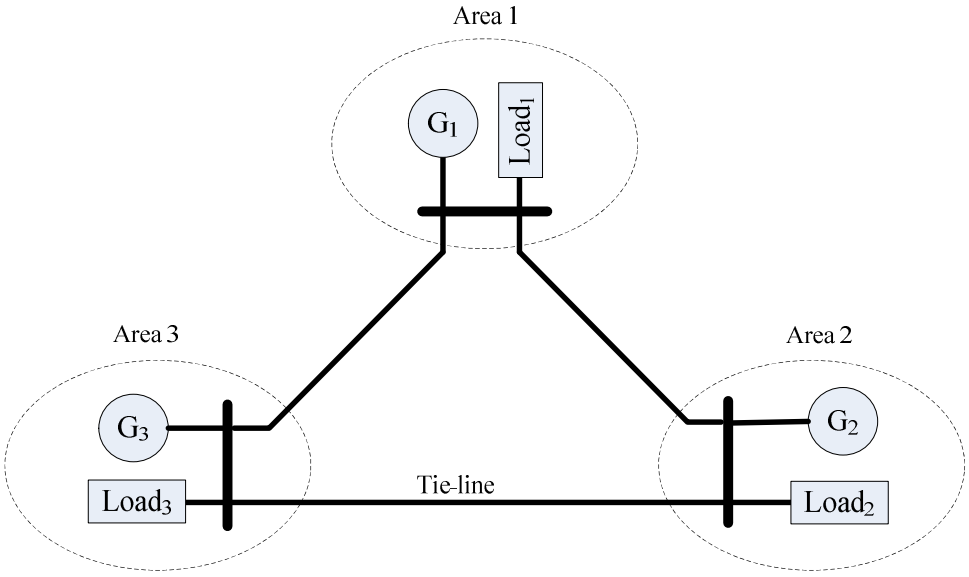

Fig. 3.10 Multi area power system configuration

Table 3.1 Parameters of the Three Area Power System

Area	D [pu/Hz]	$2H$ [pu s]	R [Hz/pu]	T_g [s]	T_i [s]	β [pu/Hz]	T_{ij} [pu/Hz]
1	0.015	0.1667	3.00	0.08	0.40	0.3483	T_{12}=0.20 T_{13}=0.25
2	0.016	0.2017	2.73	0.06	0.44	0.3827	T_{21}=0.20 T_{23}=0.12
3	0.015	0.1247	2.82	0.07	0.30	0.3692	T_{31}=0.25 T_{32}=0.12

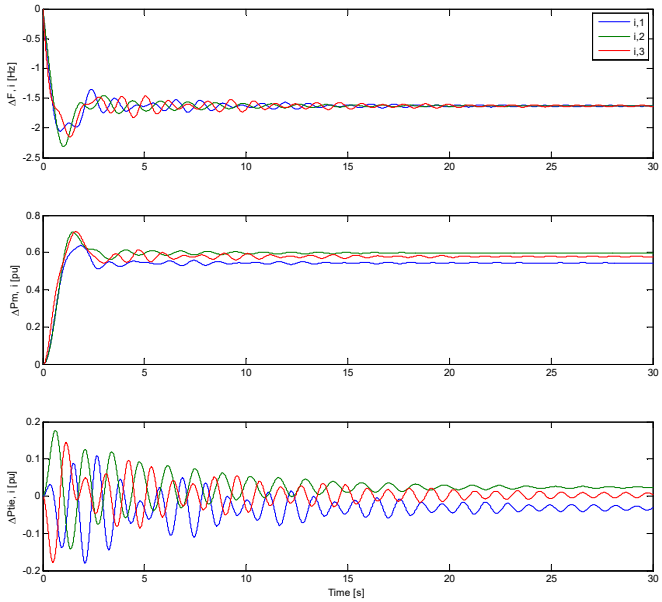

Fig. 3.11 System behavior without controller

a. Controlling System with PI Controller

PI controllers for the simulation have integral gain about -0.3, -0.2 and -0.4 for area 1 to 3 respectively and result of the simulation is captured in Fig. 3.12. Percentage overshoot (POR) and decay ratio are done by using following equations [26].

$$POR = \frac{1^{st}\ peak}{setpoint} \tag{3.31}$$

$$DR = \frac{2^{nd}\ peak}{1^{st}\ peak} \tag{3.32}$$

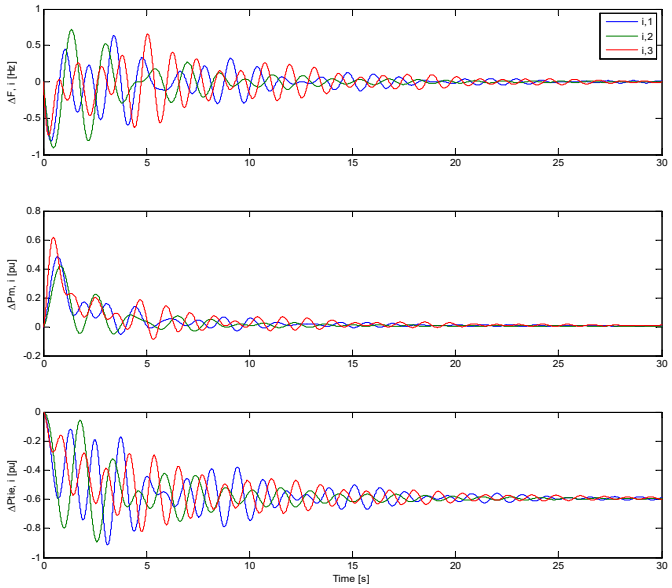

Fig. 3.12 System behavior with PI controller

Table 3.2 Properties of PI Controller Simulation

Area	F_A	F_B	F_C	*Tr*	*Tp*	*Ts*
1	50	0.4473	0.2323	0.781	1.059	0
2	50	0.7202	0.5287	0.972	1.366	0
3	50	0.6579	0.415	0.692	0.77	0

Table 3.3 Properties of PI Controller Simulation

Area	*POR*	*DR*	*USL*	*LSL*	σ	*Cp*
1	1.0089	0.5193	0.5	-0.5	0.1775	1.8779
2	1.0144	0.7341	0.5	-0.5	0.1960	1.7007
3	1.0132	0.6308	0.5	-0.5	0.1798	1.8539

The process is measured in fluctuation of ΔP_m. At this moment the step of each area will be 0.6 pu. and the measured properties of the response are given in Table 3.2. From the properties in Table 3.2, peak overshoot ratio and decay ratio can be calculated as follows.

$$POR_{PI,1} = 1 + \frac{0.4473}{50} = 1.0089$$

$$DR_{,PI,1} = \frac{0.2323}{0.4473} = 0.5193$$

In case oscillation peak about 5% is acceptable then for standard frequency 50Hz, the acceptable peak is about 1 Hz. Therefore the difference between USL and LSL is about 2 Hz.

Since the responses had center oscillation, control performance index of can be calculated using (1) and the calculations are shown in Table 3.3 as follows.

$$Cp_{PI,1} = \frac{2}{6(0.1775)} = 1.8779$$

b. Controlling System with MPC Controller

Nonlinear discrete type of MPC controllers had been built to control the power system frequency and the Laguerre function are chosen to build the MPC model. The scaling factor *a* and network lengths *N* for the model are same for each area about 0.3 and 4. Result of the simulation is shown in Fig. 3.13.

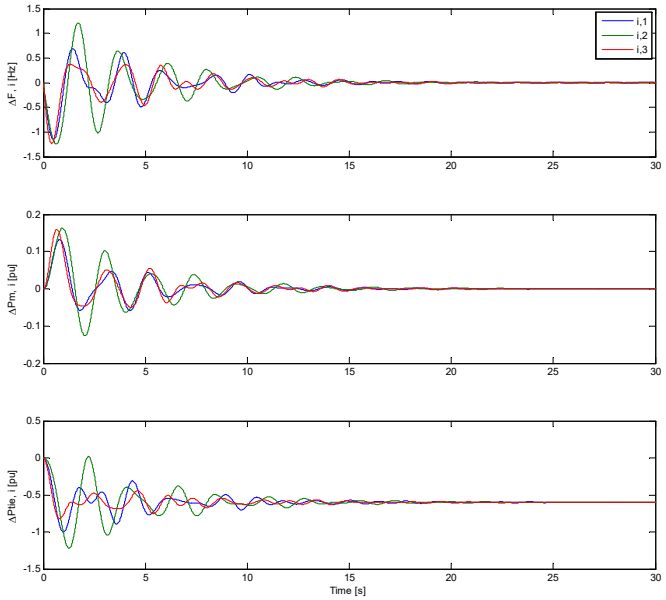

Fig. 3.13 System behavior with MPC controller

Table 3.4 Properties of MPC Controller Simulation

Area	F_A	F_B	F_C	*Tr*	*Tp*	*Ts*
1	50	0.6901	0.6086	1.039	1.444	0.675
2	50	1.2135	0.6413	1.2005	1.710	1.903
3	50	0.3777	0.3669	0.962	1.329	0.604

Table 3.5 MPC Controller Performance

Area	*POR*	*DR*	*USL*	*LSL*	σ	*Cp*
1	1.0138	0.8819	0.5	-0.5	0.2105	1.5835
2	1.0243	0.5285	0.5	-0.5	0.2987	1.1159
3	1.0076	0.9714	0.5	-0.5	0.1946	1.7129

The step about 0.6 p.u. had been applied to all area as same as in PI controller treatment. Therefore the measured properties of the response are given in Table 3.4.

Peak overshoot ratio, decay ratio and performance index of MPC controller can also be calculated using (1), (3) and (4) as follows.

$$POR_{MPC,1} = 1 + \frac{0.6901}{50} = 1.0138$$

$$DR_{,MPC,1} = \frac{0.6086}{0.6901} = 0.8819$$

$$Cp_{MPC,1} = \frac{2}{6(0.2105)} = 1.5835$$

Overall calculations can be summarized in Table 3.5. It shows that MPC controller for all area is acceptable since those have performance index more than 1.

c. Sequence Disturbance

The system is treated in long time simulations that are done with some disturbances setting in about 5 minutes (300s). The disturbances are changed every 1 minute in each area as shown in Table 3.6.

Table 3.6 Disturbance Setting (p.u.)

Area	1st	2nd	3rd	4th	5th
1	0.01	0	-0.02	0	-0.03
2	0	0.02	0	0	0.03
3	0	0	0	0.02	0

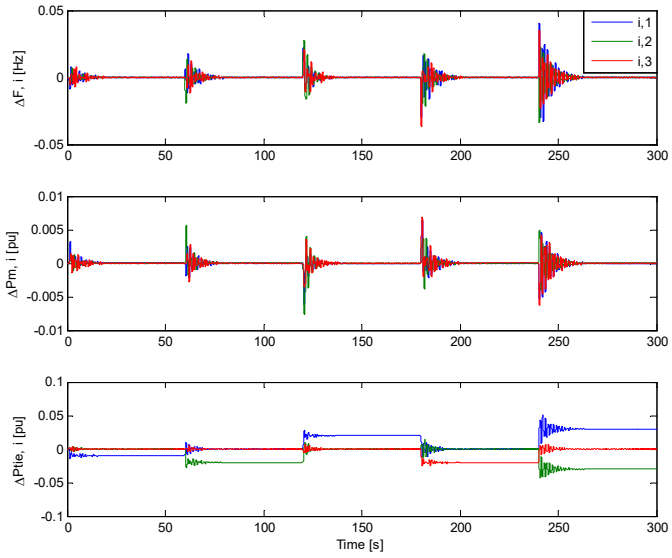

Fig. 3.14 Sequence disturbance with PI controller

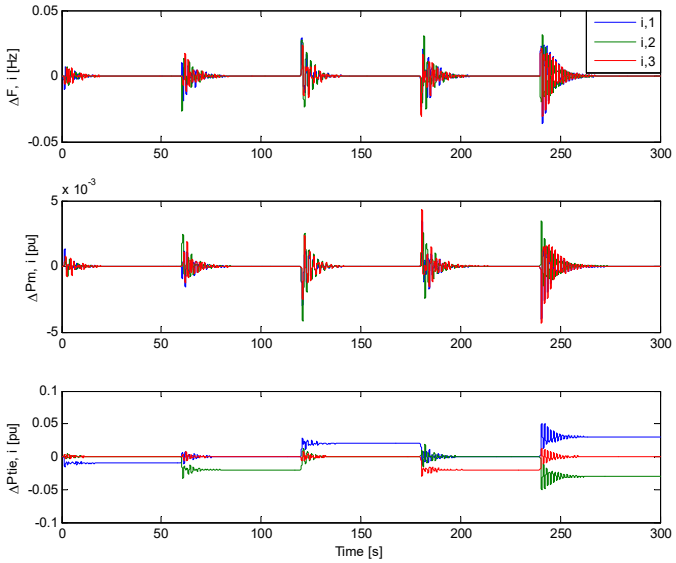

Fig. 3.15 Sequence disturbance with MPC controller

Simulation using PI controllers take about 32.7930s while using MPC controllers consume 31.8222s in CPU time. The response for long time simulations are then plotted in Fig. 3.14 and 3.15.

Both controller responses for long time simulation in Fig. 3.14 and 3.15 show that there is no significantly different in the time responses, except the prime mover deviation in the middle picture. The deviation of PI controllers had crossed 0.005 p.u. at 2^{nd}, 3^{rd}, 4^{th} and 5^{th} disturbance but MPC controllers are never passing the boundary in any disturbance.

Base on time criteria, PI controllers have the rise time and peak time faster than MPC but those are late to reach the steady state. It was shown in the settling times that have high value compared to MPC controller. From the POR and DR calculations, it can be seen that PI controllers have small POR and high DR than MPC controller have. It is means that PI controllers have little overshoots but high decay ratio. According to CPU time for long time simulation using some variation of disturbances, PI controllers consume more time to finish the simulation of three area power system. Overall it can be said that PI controllers have faster response with small overshoot but those maybe late to reach the steady state and also those need more time for completely finishing the simulation compared to MPC controller.

3.6 Summary

The basic of Load Frequency Control is introduced in this chapter. It is started by modelling the entire LFC component, including load, generator, governor, turbine and prime mover. This also introduced the concept of the effect of active power change and how the system response to the changes.

As the final part, a case study in evaluate LFC performance is shown. This case study is based on our paper in by comparing the performance of PI and MPC controller. Result of calculation shows that PI controllers have faster response than MPC controllers but MPC controllers have well decay ratio and faster in simulation time that insure the controllers to reach steady state sooner.

CHAPTER 4

ADVANCE CONTROL STRATEGY FOR LFC SYSTEM

4.1 Introduction

Control engineering has been influenced since Model Predictive Control (MPC) is proposed more than 4 decades ago. Until now the variant of MPC is increased and its performance is becoming better. In an MPC, a model of a plant is used to predict the future evolution of the process to optimize the control signal. The models used in MPC are generally intended to represent the behavior of complex dynamical systems. The advantage of an MPC is it can deal with non-linearity and a mismatch model also it has ability to predict the future behavior of the controlled plant.

In same way, an Internal Model Control (IMC) structure accommodates internal model to simulate the response of the system in order to estimate the outcome of a system disturbance. This controller uses the internal model to predict the future output of the plant and also to make correction of the output. The properties of an IMC controller are given by Garcia and Morari in [31] as a controller with dual stability criterion, zero offset and prefect control. Dual stability criterion means that in the case of the model is exact; controller and plant stability is enough to ensure overall system stability. In the absence of time delay(s) and nonminimum phase behavior this controller would be a perfect controller. The controller will reach zero offset when controller transfer function is equal with the invers of model transfer function at first step time. The difference with MPC is the internal model in an IMC is structured as an efferent model of the plant.

Due to the mismatching model, both IMC and MPC controllers may not satisfy the controller performances. Therefore it will be a challenge to provide an MPC with a great model and an adaptive model will be a solution to find the best model of the plant and to improve the controller performances.

In this chapter the adaptive models are built based on system identification methods i.e. Least Square Method, Prediction Error Minimization and Extreme Learning Machine. An IMC structure is used to find the goal by combining an adaptive internal model with an MPC.

4.2 Model Predictive Control (MPC)

The objective of the predictive control is to compute the manipulated variable u in order to optimize the output behavior of a controlled plant y. An MPC will use its internal model to calculate the manipulated variable [32].

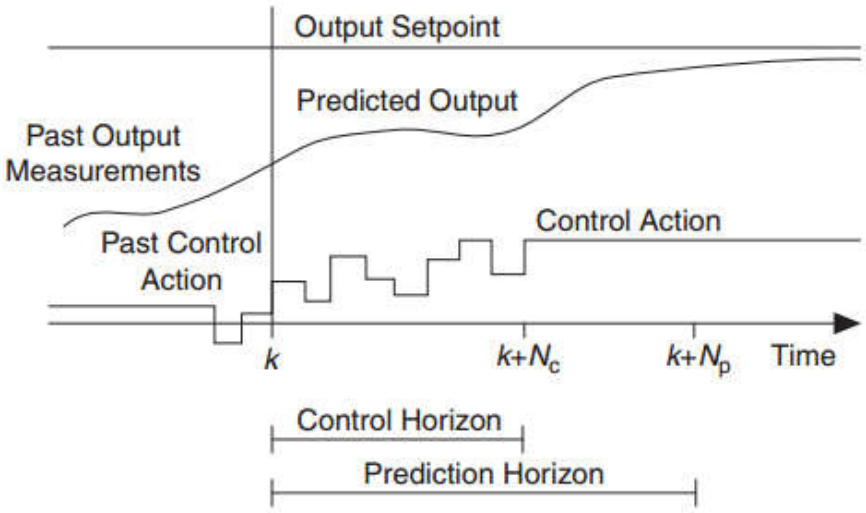

Fig. 4.1 MPC operation

At time k the MPC controller predicts the plant output for time $k+Np$. The output is optimized using objective function that normally in quadratic form. A general objective function can be shown as [32]:

$$J(k) = \sum_{m=1}^{Np} [\hat{y}(k+m \mid k) - r(k+m \mid k)]^T Q\, [\hat{y}(k+m \mid k) - r(k+m \mid k)] + \ldots$$
$$+ \sum_{m=1}^{Nc} \Delta u(k+m \mid k)^T R\, \Delta u(k+m \mid k) + \sum_{m=1}^{Np} u(k+m \mid k)^T N\, u(k+m \mid k) \qquad (4.1)$$

Where k is discrete time, N is the control action error weight matrix, Np is the number of samples in the prediction horizon, Nc is the control horizon, Q is the output error weight matrix, R is the rate of change in control action weight matrix, $\hat{y}(k+m|k)$ is the predicted plant output at time $k + m$, $r(k+m|k)$ is the output setpoint profile at time $k + m$, $\Delta u(k+m|k)$ is the predicted rate of change in control action at time $k + m$, $u(k+m|k)$ is the predicted optimal control action at time $k + m$, given all measurements up to and including those at time k.

Prediction horizon (*Np*) is expressed as the number of samples in the future during which the MPC controller predicts the plant output while control horizon (*Nc*) is the number of samples within the prediction horizon during which the MPC controller can affect the control action. By setting appropriate prediction horizon (*Np*) and control horizon (*Nc*), the MPC controller can work accurate and give optimal result. On the other hand, it can result in a not optimal controller with high overshoot.

The effect of both prediction and control horizons can be explain in a simple auto-driver car control system. For a short prediction horizon, the controller will receive not sufficient information about road, slope and speed limit that result in the lack of the controller ability for providing the correct amount of gasoline to the engine. This ability may increase for long prediction horizon increases, but this may yield to extra time need for calculation that will cause the reduction in controller performance. For the effect of control horizon to the controller performance, if the control horizon is short, the controller may reach the velocity setpoint by changing the small amount of gasoline in a few times. In a short control horizon, the controller may generate a large control action that may overshoot the velocity setpoint after the control horizon ends. In opposition, a long control horizon will cause the aggressive controller that result in oscillation and/or wasted energy. If the control horizon is set too long, the wastes of gasoline happen due to constant accelerating and decelerating. As the control action will not change after the control horizon ends, the gasoline to the engine is flown in constant so that velocity is kept changing until it reaches the setpoint.

4.2.1 Classical MPC

Model Predictive Control (MPC) is a popular optimal control scheme which is widely used in both industry and academia. This scheme works by predicting the output from the system model and attempt to the minimize error and change in control effort via an optimization process.

For a given a linear system in continues time:

$$\dot{x} = Ax + Bu \tag{4.2}$$

For discrete system with sampling time *t*, this equation can be expressed as follows.

$$x(k+1) = Ax(k) + Bu(k) \tag{4.3}$$

$$y(k) = Cx(k) \tag{4.4}$$

Then the model will be converted to augmented model so that later the QP problem respect to ΔU could be formed easily. Because $u(k)=u(k-1) + \Delta u(k)$, then the equation (4.3) can be rewritten as in (4.5) and its state space from is given in (4.6) and (4.7) [33].

$$x(k+1) = Ax(k) + Bu(k-1) + B\Delta u(k) \tag{4.5}$$

$$\begin{bmatrix} x(k+1) \\ u(k) \end{bmatrix} = \begin{bmatrix} A & B \\ 0 & 1 \end{bmatrix} \begin{bmatrix} x(k) \\ u(k-1) \end{bmatrix} + \begin{bmatrix} B \\ 1 \end{bmatrix} \Delta u(k) \tag{4.6}$$

$$y(k) = \begin{bmatrix} C & 0 \end{bmatrix} \begin{bmatrix} x(k) \\ u(k-1) \end{bmatrix} \tag{4.7}$$

For the *Np* prediction horizon based on the above equation model, the output of the prediction could be written as:

$$\begin{bmatrix} \hat{y}(k+1) \\ \hat{y}(k+2) \\ \vdots \\ \hat{y}(k+Np) \end{bmatrix} = \begin{bmatrix} CA \\ CA^2 \\ \vdots \\ CA^{Np} \end{bmatrix} x(k) + \begin{bmatrix} CB \\ CAB + CB \\ \vdots \\ \sum_{i=0}^{Np-1} CAB \end{bmatrix} u(k-1) + \cdots$$

$$\cdots + \begin{bmatrix} CB & 0 & \cdots & 0 \\ CAB + CB & CB & \cdots & 0 \\ \cdots & \cdots & \cdots & \cdots \\ \sum_{i=0}^{Np-1} CAB & \sum_{i=0}^{Np-2} CAB & \cdots & CB \end{bmatrix} \begin{bmatrix} \Delta u(k+1) \\ \Delta u(k+2) \\ \vdots \\ \Delta u(k+Np) \end{bmatrix} \tag{4.8}$$

Equation (4.8) can be simplified as in (4.9).

$$\hat{Y} = \Omega X + \Pi u + G\Delta U = F + G\Delta U \tag{4.9}$$

Then the objective function could be written as:

$$
\begin{aligned}
J &= \left(\widehat{Y} - r\right)^T \left(\widehat{Y} - r\right) + \lambda \Delta U^T \Delta U \\
&= \left(F + G\Delta U - r\right)^T \left(F + G\Delta U - r\right) + \lambda \Delta U^T \Delta U \\
&= \Delta U^T (G^T G + \lambda I)\Delta U + 2\Delta U^T G^T \left(F - r\right)
\end{aligned} \tag{4.10}
$$

Therefore, it is a QP problem which could be solved efficiently.

4.2.2 Laguerre Function Based MPC

Laguere function is built from its network that mainly applied in the system identification study. The Laguerre network is primarily built in continuous time using following equation [33].

$$
l_i(t) = \sqrt{2p}\,\frac{e^{pt}}{(i-1)!}\frac{d^{i-1}}{dt^{i-1}}\left[t^{i-1}e^{-2pt}\right] \eta = -\Omega^{-1}\Psi \mathrm{x}(t) \tag{4.11}
$$

Laguerre function can be built from the eq. (4.11) but also by making transformation for the equation. In discete time, this equation can be transformed based on z and Laplace transformation in eq. (4.12) and eq. (4.13) respectivelly.

$$
\Gamma_N(z) = \frac{\sqrt{1-a^2}}{1-az^{-1}}\left(\frac{z^{-1}-a}{1-az^{-1}}\right)^{N-1} \tag{4.12}
$$

$$
L_i(s) = \int_0^\infty l_i(t)e^{-st}dt = \frac{\sqrt{2p(s-p)^{i-1}}}{(s+p)^i} \tag{4.13}
$$

Where i=N=1...∞ is the length of Laguerre network and a or p is called time scaling factor. The scaling factor plays an important role in the Laguerre functions, which determines their exponential decay rate. It is used as a design parameter that the user will specify as part of the design requirement. Some trial in discrete time determines that for long network, the model will be more accurate but as the consequence it will build big matrices to provide the networks calculation.

Laguerre functions can be derived by constructing its state-space form as follows. If the state vector $L(t) = [l_1(t)\ l_2(t)\ \ldots\ l_N(t)]^T$ and initial conditions of the state vector $L(0) = \sqrt{2p}[1\ 1\ \ldots\ 1]^T$, the Laguerre functions will be:

$$
L(k+1) = A_l L(k) \tag{4.14}
$$

Where :

$$A_l = \begin{bmatrix} a & 0 & 0 & 0 & \cdots & 0 \\ \alpha & a & 0 & 0 & \cdots & 0 \\ -a\alpha & \alpha & a & 0 & \cdots & 0 \\ a^2\alpha & -a\alpha & \alpha & a & \cdots & 0 \\ \vdots & \vdots & \vdots & \vdots & \ddots & 0 \\ -a^{N-2}\alpha & -a^{N-3}\alpha & -a^{N-4}\alpha & \cdots & -a^{N-N}\alpha & a \end{bmatrix}$$

For a given state space augmented model $(\tilde{A},\tilde{B},\tilde{C})$ of Laguerre based discrete MPC at sampling time m with Δu as the input signal and initial state variable $x(k)$, the prediction of the future state variable $x(k+m|k)$ is written as (4.15) with $\phi(m)$ is in (4.16) and $\Delta u(k+i)=L(i)^T\eta$. In same way $y(k+m|k)$ the output is written in (4.17).

$$\begin{aligned} x(k+m\,|\,k) &= \tilde{A}^m x(k) + \sum_{i=0}^{m-1} \tilde{A}^{m-i-1}\tilde{B}\Delta u(k+i) \\ &= \tilde{A}^m x(k) + \sum_{i=0}^{m-1} \tilde{A}^{m-i-1}\tilde{B}L(i)^T\eta \\ &= \tilde{A}^m x(k) + \phi(m)^T\eta \end{aligned} \tag{4.15}$$

$$\phi(m) = \sum_{i=0}^{m-1} \tilde{A}^{m-i-1}\tilde{B}L(i)^T \tag{4.16}$$

$$y(k+m\,|\,k) = \tilde{C}\tilde{A}^m x(k) + \sum_{i=0}^{m-1} \tilde{C}\tilde{A}^{m-i-1}\tilde{B}L(i)^T\eta \tag{4.17}$$

Where the objective is to find the coefficient vector η to minimize the cost function:

$$J = \sum_{m=1}^{Np} x(k+m\,|\,k)^T Q x(k+m\,|\,k) + \eta^T R_L \eta \tag{4.18}$$

By substituting (4.16) into (4.18), the cost function will become (4.19)

$$\begin{aligned} J = {} & \eta^T\left(\sum_{m=1}^{Np}\phi(m)Q\phi(m)^T + R_L\right)\eta + 2\eta^T\left(\sum_{m=1}^{Np}\phi(m)QA^m\right)x(k) + \\ & \sum_{m=1}^{Np} x(k)^T(A^T)^m QA^m x(k) \end{aligned} \tag{4.19}$$

Taking partial derivative to find the minimum solution of the cost function will result to

$$\frac{\partial J}{\partial \eta} = 2\left(\sum_{m=1}^{Np}\phi(m)Q\phi(m)^T + R_L\right)\eta + 2\left(\sum_{m=1}^{Np}\phi(m)QA^m\right)x(k)$$

If $\left(\sum_{m=1}^{Np}\phi(m)Q\phi(m)^T + R_L\right)^{-1}$ exist when $\partial J/\partial \eta$ =0 then the optimal solution of the parameter vector η is defined as

$$\eta = -\frac{\left(\sum_{m=1}^{Np}\phi(m)QA^m\right)x(k)}{\left(\sum_{m=1}^{Np}\phi(m)Q\phi(m)^T + R_L\right)} = -\frac{\Psi}{\Omega}x(k) \tag{4.20}$$

Where R_L is a diagonal matrix ($m \times m$) with the penalty $r(k)$ on its diagonal, $\Omega = \sum_{m=1}^{Np}\phi(m)Q\phi(m)^T + R_L$, and $\Psi = \sum_{m=1}^{Np}\phi(m)QA^m$.

The control law with optimal gain K_{mpc} for close loop system can then be obtained in (4.21).

$$x(k+1) = (A - BK_{mpc})x(k) \tag{4.21}$$

$$K_{mpc} = L(0)^T \Omega^{-1}\Psi \tag{4.22}$$

The receding horizon control is also applied to strengthen the robustness of system so that only first sample of the control trajectory is applied as the input. The receding control is obtained by following equation

$$\Delta u = L(0)^T \eta = -K_{mpc}x \tag{4.23}$$

4.2.3 MPC with Constraints

The advantage of an MPC is the ability to deal with any constraints inside the system. The types of constraints that frequently encountered in continuous time applications are:

- Constraints on the manipulated variable rate of change, $du^{min} \leq \dot{u} \leq du^{max}$
- Constraints on the amplitude of the manipulated variable, $u^{min} \leq u(t) \leq u^{max}$
- Output Constraints, $y^{min} - s_v \leq y(t) \leq y^{max} + s_v$, where slack variable s_v is given to forming a soft constraint to avoid the instability of the controller.

a. Quadratic programming for equality constraints

The quadratic programming using Lagrange multiplier can be used to find the constrained minimum of a positive definite quadratic function with linear equality constraints as follows [33].

$$\lambda = -\left(ME^{-1}M^T\right)^{-1}\left(\gamma + ME^{-1}F\right) \tag{4.24}$$

$$x = -E^{-1}\left(M^T\lambda + F\right) \tag{4.25}$$

Where E and F are matrices taken from objective function, M and γ are forming from the equality constraints and λ is called Lagrange multiplier.

b. Primal-dual method

If there are many constraints, the computational load is quite large. A dual method can be used to identify the constraints that are not active and they can then be eliminated in the solution so that computation will be simple and the primal variable vector *x* is obtained using as follows [33].

$$x = -E^{-1}F - E^{-1}M_{act}^{T}\lambda_{act} \tag{4.26}$$

Subject to λ ≥ 0, are denoted as λ_{act}, and the corresponding constraints are described by M_{act} *and* γ_{act}.

c. Hildreth's quadratic programming procedure

This quadratic programming procedure was proposed for solving this dual problem and it can be formulated as follows [33].

$$x = -E^{-1}\left(F + M^{T}\lambda^{*}\right) \tag{4.27}$$

Where λ^{*} contains zeros for inactive constraints and the positive components corresponding to the active constraints and the positive component collected as a vector is called λ^{*}_{act} with its value defined by [33].

$$\lambda_{act}^{*} = -\left(M_{act}E^{-1}M_{act}^{T}\right)^{-1}\left(\gamma_{act} + M_{act}E^{-1}F\right) \tag{4.28}$$

4.3 Internal Model Control (IMC)

Internal model is a process model that simulates the response of the system in order to estimate the outcome of a system disturbance. An Internal Model Control (IMC) can use the internal model to predict the future output of the plant and also to make correction of the output. This controller can be used to control a plant [6], to tune other controller [7], or to combine with the other controller such as PI/PID [7]–[12], Fuzzy controller [13], [14], Neural Network [15] or MPC [15]–[17].

An IMC principle can be figured out in Fig. 4.2 with the input reference *r* will be given as the reference input to controller *Q*. The controller will respond the input by sending any command *u* to the plant *P* and as the same time it is fed to the internal/efferent model *G*. The plant then moves to the desired output *y*. In case disturbance(s) *d* happen, the signal correction *đ* as result of the desired output of

both plant and efferent model will be fed back to the controller. Control law applied for the IMC control can be written as follows [8].

$$y = PQr + (1 - GQ)d \tag{4.29}$$

$$u = Qr - Qd \tag{4.30}$$

$$e = (1 - PQ)r - (1 - GQ)d \tag{4.31}$$

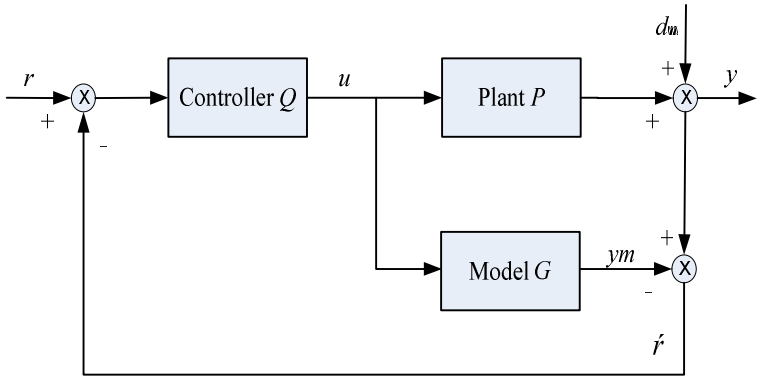

Fig. 4.2 IMC Principle

The difference between classical controller and an IMC is that an IMC will correct the actual output before it is fed back. Since an IMC uses the efferent model, the model should be a perfect model to have the highest control performance. The way to provide the model in an IMC can be in forward model, inverse models, combination of both forward and inverse models, or adaptive model.

4.4 Adaptive Control Strategy

4.4.1 Least Mean Square

Due to highly non-linearity in a power system, the classical model of power system may not accurate to configure the real power system. Therefore a simple model of a load frequency of power system is used to be used using least square method (LSM). In order to capture the essential dynamics of power system, a first order lag model of frequency deviation is expanded and implemented in least square method as follows.

$$\Delta f_{k+1} = -\frac{1}{T}\Delta f_k + \frac{K}{T}\Delta P_k = A\Delta f_k + B\Delta P_k \tag{4.32}$$

For discrete time system, the above equation can be described in a matrix form as follows.

$$\begin{bmatrix} \Delta f_{1,k+1} \\ \vdots \\ \Delta f_{N,k+1} \end{bmatrix} = \begin{bmatrix} A_{1,1} & \cdots & A_{1,N} \\ \vdots & \ddots & \vdots \\ A_{N,1} & \cdots & A_{N,N} \end{bmatrix} \begin{bmatrix} \Delta f_{1,k} \\ \vdots \\ \Delta f_{N,k} \end{bmatrix} + \begin{bmatrix} B_{1,1} & \cdots & B_{1,N} \\ \vdots & \ddots & \vdots \\ B_{N,1} & \cdots & B_{N,N} \end{bmatrix} \begin{bmatrix} \Delta P_{1,k} \\ \vdots \\ \Delta P_{N,k} \end{bmatrix} \quad (4.33)$$

Consider a linear equation of least square method $y=Hx$, a solution for minimizing the error can be written as:

$$J(x) = \|y - Hx\|^2 \quad (4.34)$$

Then expanding $J(x)$ gives

$$\begin{aligned} J(x) &= (y - Hx)^T (y - Hx) \\ &= y^T y - y^T Hx - x^T H^T y + x^T H^T Hx \\ &= y^T y - 2y^T Hx + x^T H^T Hx \end{aligned}$$

Taking the derivative for the $J(x)$ gives

$$\frac{\partial}{\partial x} J(x) = -2H^T y + 2H^T Hx \quad (6)$$

Minimizing the derivative by setting it to zero gives

$$H^T Hx = H^T y \quad (4.35)$$

In case of H^TH is invertible, the LSM solution is given by

$$x = \left(H^T H\right)^{-1} H^T y \quad (4.36)$$

Where $(H^TH)^{-1}H^T$ is pseudo inverse of H matrix. By substituting the discrete time equation of power system model into a linear system equation we get

$$\begin{bmatrix} \Delta f_{1,k+1} \\ \vdots \\ \Delta f_{N,k+1} \end{bmatrix} = \begin{bmatrix} \Delta f_{1,k} & \cdots & \Delta f_{N,k} & \Delta P_{1,k} & \cdots & \Delta P_{N,k} \\ \vdots & \ddots & \vdots & \vdots & \ddots & \vdots \\ \Delta f_{1,k+m-1} & \cdots & \Delta f_{N,k+m-1} & \Delta P_{1,k+m-1} & \cdots & \Delta P_{N,k+m-1} \end{bmatrix} \begin{bmatrix} A_{i,1} \\ \vdots \\ A_{i,N} \\ B_{i,1} \\ \vdots \\ B_{i,N} \end{bmatrix} \quad (4.37)$$

Power system input power ΔP and power system frequency Δf is selected as input and output for the model.

4.4.2 Prediction Error Minimization (PEM)

As proposed in this research, an adaptive model will be used to provide a perfect model of the plant. Along the simulation, the adaptive model is built by utilizing input and output data. Then the model is generated to a state space model.

In order to realize the adaptive model in MATLAB environment, the state space model can be estimated using `ssest` command. Using this command, a state space model can be generated from a given system identification data by using prediction error minimization (PEM) algorithm. A numerical optimization is used by the PEM algorithm to minimize the cost function. Recently the PEM algorithm in MATLAB environment is only provided with the cost function as follows [34].

$$V_N(G,H) = \sum_{t=1}^{N} e^2(t) \tag{4.38}$$

Where *e(t)* is the difference between the measured output and the predicted output *G* of the model with *N* number of samples.

4.4.3 Extreme Learning Machine (ELM)

An ELM is basically a single hidden layer feed-forward neural network (SLFN) which has an excellent training algorithm. Input weight and hidden layer biases are not necessarily adjusted and those can be chosen arbitrarily in this algorithm. Then the output weight of the SLFNs can be determined by a generalized inverse operation of the hidden layer output matrices. In fact, this procedure has been fastening this algorithm.

For a given $\tilde{n}$ training set samples (x_j, t_j) where $x_j=[x_{j1}, x_{j2},..., x_{j\tilde{n}}]^T$ and $t_j=[t_{j1}, t_{j2},..., t_{j\tilde{n}}]^T$, an SLFN with $\tilde{N}$ hidden neurons and activation function *g(x)* is expressed as [24], [35], [36].

$$\sum_{i=1}^{\tilde{N}} \beta_i' g(x_j) = \sum_{i=1}^{\tilde{N}} \beta_i' g(w_i x_j + b_i) = o_j, j = 1,2,...,\tilde{n} \tag{4.39}$$

Where $w_i=[w_{i1}, w_{i2},..., w_{i\tilde{n}}]^T$, $\beta'_i=[\beta'_{i1}, \beta'_{i2},..., \beta'_{i\tilde{n}}]^T$, b_i, and o_j are the connecting weight of i^{th} hidden neuron to input neuron, the connecting weights of the i^{th} hidden neuron to the output neurons, the bias of the i^{th} hidden node, and the actual network output with respect to input x_j respectively. Because the standard SLFN can minimize the error between t_j and o_j, eq.(4.39) can be rewritten as follows.

$$\sum_{i=1}^{\tilde{N}} \beta_i' g(w_i x_j + b_i) = t_j, j = 1,2,...,\tilde{n} \quad (4.40)$$

In simple (4.40) can be $H\beta'=T$ so that the output weight matrix β' can be solved by least square solution as in (4.41).

$$\beta'=H^{\dagger}T \quad (4.41)$$

The hidden layer output matrix H and the network output T are formulated as follows.

$$H\left(w_i,b_i\right)=\begin{bmatrix} g(w_1 x_1 + b_1) & \cdots & g(w_{\tilde{N}} x_1 + b_{\tilde{N}}) \\ \vdots & \cdots & \vdots \\ g(w_1 x_{\tilde{n}} + b_1) & \cdots & g(w_{\tilde{N}} x_{\tilde{n}} + b_{\tilde{N}}) \end{bmatrix}, \text{ and } \quad T=\begin{bmatrix} t_1^T \\ \vdots \\ t_{\tilde{n}}^T \end{bmatrix} \quad (4.42)$$

4.5 Case Studies

4.5.1 IMC using PEM method

An adaptive IMC model is tested in a three area power system to test the effectiveness of the proposed controller. The decision is based on variables needs and also time consuming for the simulation. Therefore this simulation can be extended to a larger area power system under consequence for the long simulation time. The configuration of investigated multi-area power system is depicted in Fig. 3.10. The power system configuration is based on [2], [24]–[27] and its parameter as shown in Table 3.1. while the system dynamics are figured in Fig. 3.7. Simulations were done in three cases as in [27] which are with step disturbance and some noises, without disturbance and very high noises, and with mismatch model in point a-c as follows.

a. Case I: Step Disturbance

Nonlinear discrete type of MPC controller is built to control the power system frequency and the Laguerre function is chosen to build the MPC model. The scaling factor a and network lengths N for the model are same for each area about 0.3 and 4.

The step about 0.2 pu and disturbances with maximum 0.1 pu of the generator capacity are applied to area 1 to 3. Therefore the measured properties of the response are given in table IV while the simulation result is shown in Fig. 4.3.

An adaptive IMC-MPC scheme has been built to be applied to the system. In this case the model will be updated each second with the input output data. The data

is then used to build the adaptive model. With the same treatment as in MPC controller, the adaptive IMC-MPC simulation result is shown in Fig. 4.4.

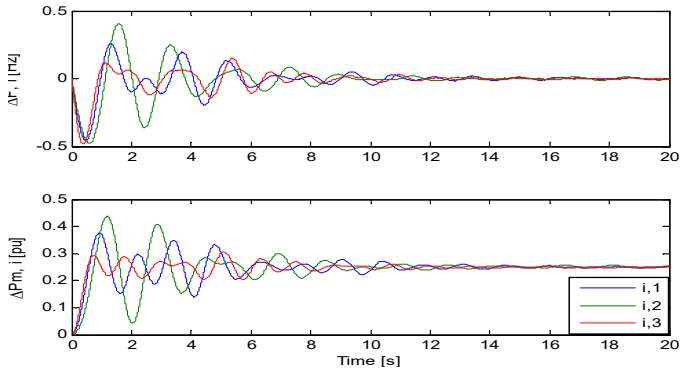

Fig. 4.3 Fig. 1.MPC controller responses in case I

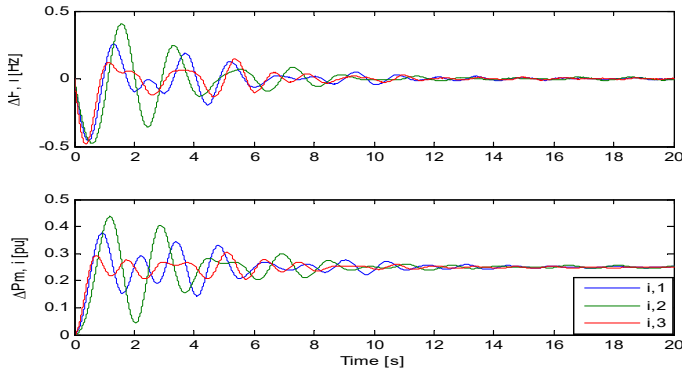

Fig. 4.4 Adaptive IMC-MPC controller responses in case I

b. Case II: Very High Noises

The MPC and IMC-MPC are then used in another case with very noisy. In this case I, the step disturbance is set to zero and a random about maximum 0.5 pu of the generator capacity is applied to all areas. Responses of the both controller are then figured in Fig. 4.5 for MPC and Fig. 4.6 for IMC-MPC.

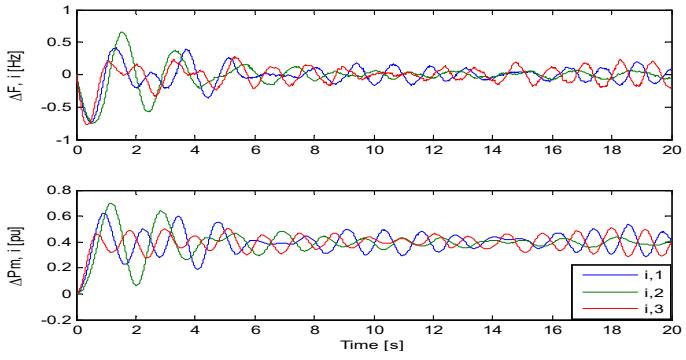

Fig. 4.5 MPC controller responses in case II

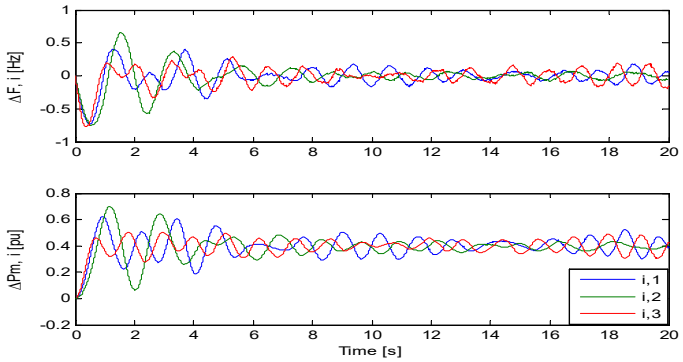

Fig. 4.6 Adaptive IMC-MPC controller responses in case II

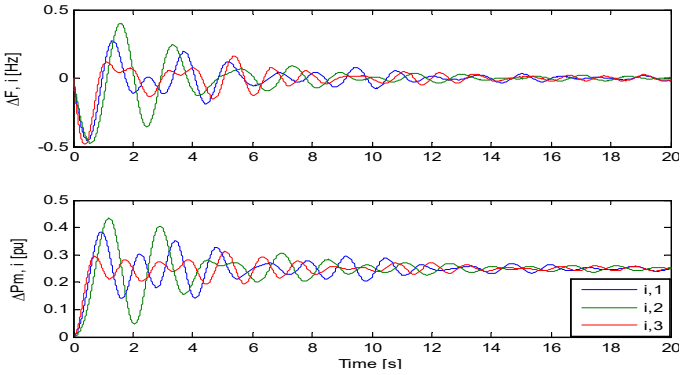

Fig. 4.7 MPC controller responses in case III

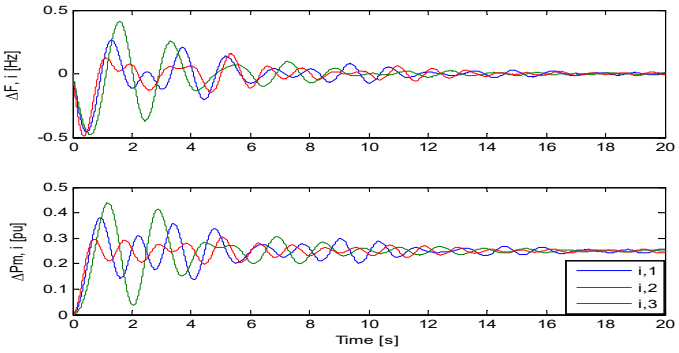

Fig. 4.8 Adaptive IMC-MPC controller responses in case III

c. Case III: Mismatch Model

In this case, a mismatch model is applied to all areas in term of governor time constant. The time constant is change for each area generator by increasing (area 1 and 3) and decreasing (area 2) its values by 0.01s. After the changes, the system is then tested with a 0.2 pu. step disturbance for all areas. Result for the system responses is figured in Fig. 4.7 and 4.8 for MPC and IMC-MPC respectively.

d. Performance Evaluation

Base on system response in Fig. 4.3 to 4.8, the overshoot decay ration and standard deviation are analyzed and the result is provided in Table 4.1 and Table 4.2. For case I and II, IMC-MPC controller gives very good response in area 1 and 3. On the other hand IMC-MPC controller is superior in all area of case III. On the other hand IMC-MPC controller has high decay ratio in most area and cases which indicate that this controller can slowly reduce the frequency deviation.

Table 4.1 Frequency Deviation Analysis

	Area	MPC			IMC-MPC		
		case I	case II	case III	case I	case II	case III
Overshoot	1	0.2582	0.4128	0.2738	0.2574	0.4115	0.2737
	2	0.4049	0.6605	0.4025	0.4049	0.6608	0.4024
	3	0.1191	0.2037	0.1643	0.1181	0.2026	0.1614
Decay Ratio	1	0.7378	0.9617	0.7213	0.7570	0.9779	0.7850
	2	0.6090	0.5687	0.6104	0.6153	0.5687	0.6192
	3	0.3168	0.8391	0.4802	0.3391	0.6935	0.3995
Standard Deviation	1	0.0916	0.1673	0.0943	0.0921	0.1665	0.0938
	2	0.1233	0.1976	0.1229	0.1234	0.1975	0.1223
	3	0.0808	0.1581	0.0847	0.0809	0.1532	0.0844

Table 4.2 Prime Mover Deviation Analysis

	Area	MPC			IMC-MPC		
		case I	case II	case III	case I	case II	case III
Overshoot	1	0.1465	0.2354	0.1464	0.1441	0.2321	0.1004
	2	0.1729	0.2713	0.1718	0.1719	0.2709	0.1209
	3	0.1652	0.2649	0.1661	0.1612	0.2597	0.1195
Decay Ratio	1	0.9156	0.9633	0.9142	0.9254	0.9722	0.9406
	2	0.8937	0.8728	0.9081	0.8940	0.8712	0.9077
	3	0.9149	0.9239	0.9386	0.9164	0.9746	0.9240
Standard Deviation	1	0.0294	0.0531	0.1464	0.0318	0.0504	0.2738
	2	0.0443	0.0710	0.1718	0.0466	0.0691	0.4024
	3	0.0278	0.0534	0.1661	0.0700	0.0500	0.1614

About prime mover deviation, IMC-MPC controller has perfect overshoot in all areas and all cases comparing to the MPC controller. It is also shown that IMC-MPC controller is more dynamic than MPC controller as it has high standard deviation and decay ratio values.

4.5.2 IMC using ELM method

The power system configuration for testing the proposed controller is based on [2], [24]–[27] and the parameters as shown in Table 3.1 while the system dynamics are figured in Fig. 3.7. Simulations were done in two cases and the simulation setup is configured in Table 4.3, where step and random disturbance are imposed on the load in all area as in [24]. The random disturbance implies load changes of white noise with a maximum 0.1 pu while step disturbance is assumed as load change in constant for a certain time.

Table 4.3 Simulation Setup

Case	Step Disturbance [pu]	Random Disturbance [pu]
I	0.2	0.1
II	0.2	-

A Laguerre function based MPC controller is built to control a three area power system frequency. To ensure the MPC stability, the scaling factor a is tuned to 0.1 while network lengths N is set to 4 for each area controller. The model will be updated each second with the input-output data using ELM method. Overall simulation responses of frequency and mechanical power deviation for both existing and proposed controller are plotted in Fig. 4.9 and 4.10.

The controller performance is evaluated based on system responses and signal measures. Standard deviation is also provided to indicate how sensitive the controller to response the errors.

For the system responses based evaluation, overshoot and standard deviation are analyzed and the results are provided in Table 4.4 as well as its visual in Fig. 4.11 and 4.12 based on system responses in Fig. 4.9 and 4.10. According to the figures and table, it can be simply known that the proposed controller has very good response overshoot of frequency and mechanical power compared to the existing MPC controller in all areas of both cases. On the other hand, the proposed controller

slightly aggressive to the disturbances as shown in high standard deviations in some areas and cases. These are the evidence that the proposed controller can accurately cover the power system dynamics and also it shows the ability to increase controller performance by sending proper feedback to the controller by utilizing the adaptive model.

By the treatment as same as in the case I, the other adaptive internal model for LFC application introduced in [27] has overshoot responses 0.1465, 0.1729, and 0.1652 and standard deviation 0.0294, 0.0443, and 0.0278 for area 1-3 respectively. Compared to the proposed controller, it is proved that the proposed controller has smaller overshoot and higher standard deviation compared. These are the indications that the proposed controller is more active to maintain the frequency change during the simulation and so it only has a small overshoot on the simulation.

Table 4.4 Frequency and Mechanical Power Deviation Analysis

	Area	Frequency Deviation				Mechanical Power Deviation			
		MPC Cases		Adaptive IMC Cases		MPC Cases		Adaptive IMC Cases	
		I	II	I	II	I	II	I	II
Overshoot	1	0.1346	0.2190	0.0923	0.2047	0.3437	0.3401	0.3080	0.3109
	2	0.0860	0.1162	0.0407	0.1147	0.4164	0.4165	0.3473	0.3484
	3	0.1374	0.2530	0.1259	0.2384	0.4605	0.4625	0.4318	0.4340
Standard Deviation	1	0.1762	0.1967	0.1767	0.1946	0.0372	0.0428	0.0442	0.0814
	2	0.1786	0.1838	0.1795	0.1842	0.0418	0.0432	0.0354	0.0514
	3	0.1714	0.2012	0.1714	0.1976	0.0522	0.0580	0.0450	0.0738

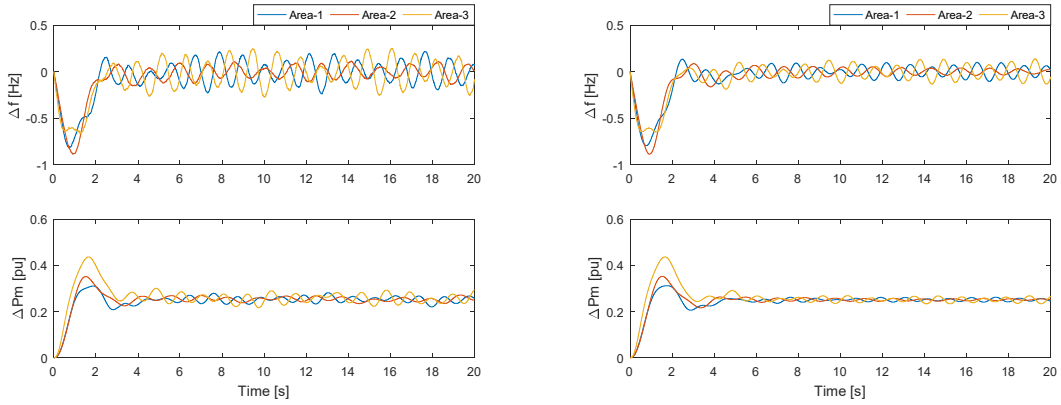

(a) (b)

Fig. 4.9 MPC controller responses (a) Case I and (b) Case II

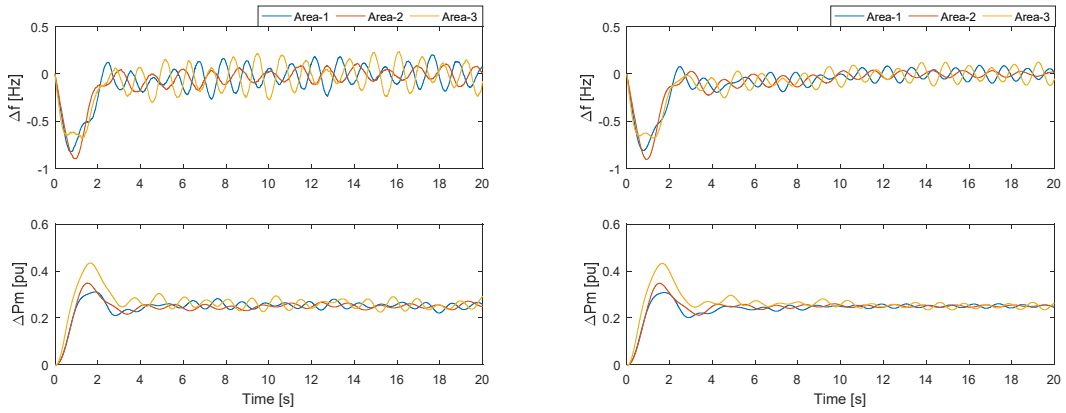

(a) (b)

Fig. 4.10 Adaptive IMC controller responses (a) Case I and (b) Case II

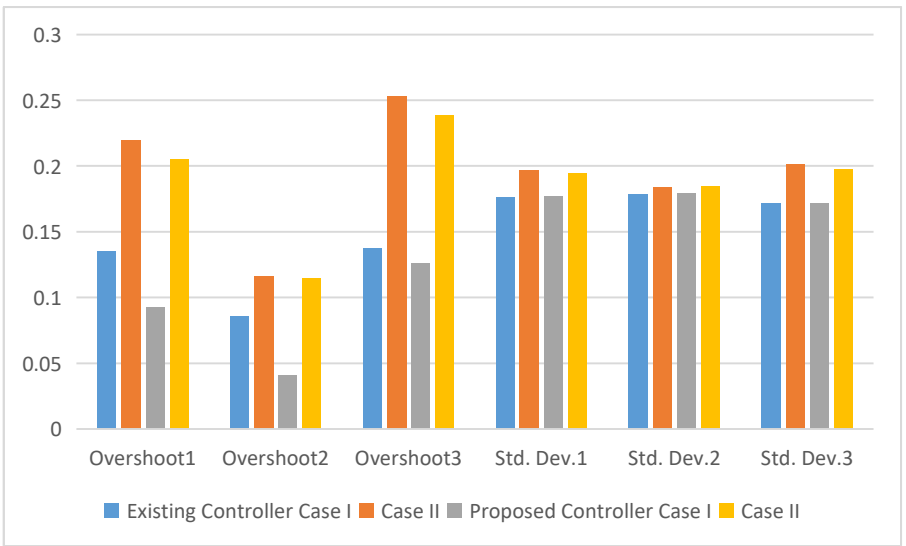

Fig. 4.11 Frequency deviation

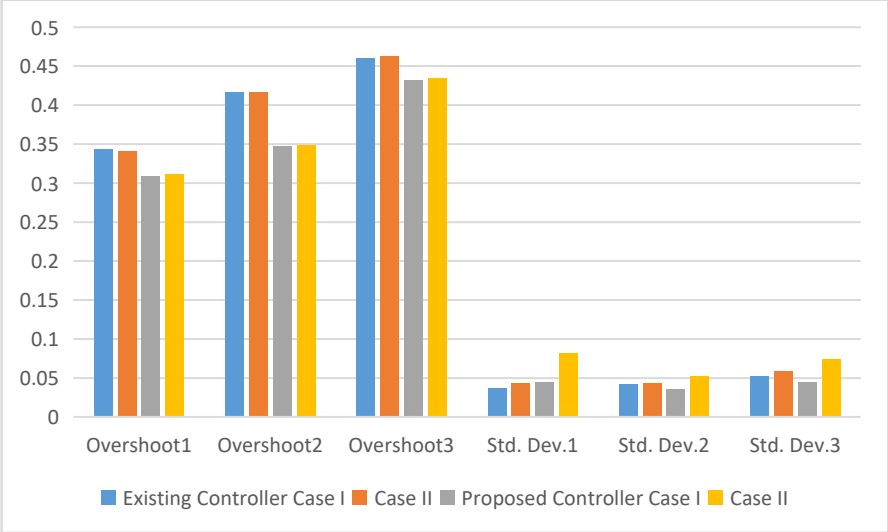

Fig. 4.12 Mechanical power deviation

The signal measured based evaluation of the proposed controller including Integral of the absolute value of the error (IAE), Integral of the square value of the error (ISE) and Integral of the time-weighted absolute value of the error (ITAE) are provided in Table 4.5. It is shown that the proposed controller has small errors in IAE and ITAE index while it has high deviation in the ISE index in both cases. These are the validation that the proposed controller has no persisting high errors and it adaptively follows the load changes in the simulation.

The specifications of the machine to run the simulation runs are Intel Core i7 2.9 GHz CPU and 16 GB RAM using MatLab 2016a under Windows 10 environment. CPU time for both cases of MPC, and case I and II of adaptive IMC are 1.5509, 1.5446, 6.6927 and 6.4599 seconds respectively. It seems like the proposed controller will need time 4 times longer than the existing controller since it needs to build its own model in a certain period which is in this cases every second. This may not degrade the performance in real operation since the CPU time is still littler than simulation setting time.

Table 4.5 Controller Index Analysis

	Area	MPC			Adaptive IMC		
		IAE	ISE	ITAE	IAE	ISE	ITAE
Case I	1	1.9340	0.6858	10.6362	1.9039	0.6900	10.1068
	2	1.6508	0.7028	6.9319	1.6532	0.7118	6.8517
	3	2.1407	0.6593	14.1713	2.0966	0.6589	13.4449
	avg	1.9085	0.6827	10.5798	1.8846	0.6869	10.1345
Case II	1	2.2608	0.7425	15.0622	2.2289	0.7444	14.4818
	2	1.6748	0.7204	6.8818	1.6792	0.7297	6.8696
	3	2.6418	0.7685	20.5055	2.5884	0.7626	19.6189
	avg	2.1924	0.7438	14.1498	2.1655	0.7456	13.6567

4.6 Summary

This section proposed a new adaptive control to be applied in an LFC system. It starts by introducing Model Predictive Control in classical and enchanting to Laguerre based MPC. Internal Model Control (IMC) is also described in this section as its structure is used in the proposed controller.

To setup the proposed controller as an adaptive controller, the system identification method is applied. This identification method is based on Least Square Method, Prediction Error Minimization and Extreme Learning Machine. The effectiveness of this methods is tested and simulated in the case studies.

Finally case studies are given in the last part of this section. This cases studies are used to simulated our proposed methods in a power system. Based on this case studies, It is assumed that our proposed controller can work to handle the frequency dynamics in a power system better than the conventional controllers.

CHAPTER 5

CONCLUSIONS AND FUTURE RESEARCH

5.1 Conclusions

This thesis present an advanced controller based on Adaptive Model Predictive Control. This controller is introduced to control Load Frequency of power systems. The adaptive controller is achieve by system identification method.

Some methods in system identification have been proposed to increase the adaptive control performance, including Least Square Method, Prediction Error Immunizations and Extreme Learning Machine. The controller performance is evaluated based on peak criteria of system response and also controller index.

A three area power system is chosen to validate the controller in handling load frequency control including step and random disturbance. Results of the simulation show that the proposed controller can accurately handle the power system dynamics. Furthermore, the proposed controller can effectively reduce the frequency and mechanical power deviation under disturbances of the power system.

5.2 Future Work

The proposed controller is still being identification, some system identification method will be introduced to reached high performance controller in real time simulation. Additionally, the load or disturbance have to be more sophisticated model to simulate environment closer to a real system. As the usage renewable technology continues to increase, future research should take into account photovoltaic and wind farm penetration in a large power system.

ICW 2018
TELKOMNIKA

2018 1st INTERNATIONAL CONFERENCE AND WORKSHOP ON
TELECOMMUNICATION, COMPUTING,
ELECTRICAL, ELECTRONICS AND CONTROL

Universitas Ahmad Dahlan (UAD)

September 18-21, 2018 | Royal Ambarrukmo Hotel, Yogyakarta, Indonesia

BEST PAPER AWARD

Awarded to:

Adelhard Beni Rehiara, He Chongkai, Yutaka Sasaki, Naoto Yorino, Yoshifumi Zoka

For the paper entitled:

An Adaptive Internal Model for Load Frequency Control Using Extreme Learning Machine

Tole Sutikno, Ph.D.
Director, LPPI UAD

Anton Yudhana, Ph.D.
Conference Chair

REFERENCES

[1] A. B. Rehiara, “Transient Stability of SMIB : a Case Study,” in *Conference on Information Technology and Electrical Engineering (CITEE 2009)*, 2009, pp. 12–16.

[2] T. H. Mohamed, A. A. Hassan, H. Bevrani, and T. Hiyama, “Model Predictive Based Load Frequency Control Design,” in *16th International Conference on Electrical engineering*, 2010.

[3] A. M. Ersdal, L. Imsland, and K. Uhlen, “Model Predictive Load-Frequency Control,” *IEEE Trans. Power Syst.*, vol. 31, no. 1, pp. 777–785, 2016.

[4] S. K. Jain, A. Bhargava, and R. K. Pal, “Three area power system load frequency control using fuzzy logic controller,” in *International Conference on Computer, Communication and Control*, 2015, pp. 1–6.

[5] L. Cai, Z. He, and H. Hu, “A New Load Frequency Control Method of Multi-Area Power System via the Viewpoints of Port-Hamiltonian System and Cascade System,” *IEEE Trans. Power Syst.*, vol. 32, no. 3, pp. 1689–1700, 2017.

[6] F. Liping and W. Xiyang, “Internal model based iterative learning control for linear motor motion systems,” *Proc. - ISDA 2006 Sixth Int. Conf. Intell. Syst. Des. Appl.*, vol. 3, pp. 62–66, 2006.

[7] W. K. Ho, T. H. Lee, H. P. Han, and Y. Hong, “Self-tuning IMC-PID control with interval gain and phase margins assignment,” *IEEE Trans. Control Syst. Technol.*, vol. 9, no. 3, pp. 535–541, 2001.

[8] T. Shigemasa, M. Yukitomo, and R. Kuwata, “A model-driven PID control system and its case studies,” *Proc. Int. Conf. Control Appl.*, vol. 1, pp. 571–576, 2002.

[9] H. Seki, “Adaptive IMC-PI controllers for process applications,” *12th IEEE Int. Conf. Control Autom.*, pp. 455–460, 2016.

[10] J.-J. Gu, L. Shen, and L.-Y. Zhang, “Application of internal model and self-adaptive PSD controller in the main steam temperature system,” *2005 Int. Conf. Mach. Learn. Cybern. Icmlc 2005*, no. August, pp. 570–573, 2005.

[11] Y. Baba, T. Shigemasa, M. Yukitomo, F. Kojima, M. Takahashi, and E. Sasamura, “Model-driven PID control system in single-loop controller,” *Proc. SICE 2003 Annu. Conf*, vol. 1, pp. 187–190, 2003.

[12] M. Shamsuzzoha and M. Lee, “IMC Based Control System Design of PID Cascaded Filter,” *SICE-ICASE Int. Jt. Conf. 2006*, vol. Oct. 18-2, pp. 2485–2490, 2006.

[13] Q. Jin, C. Feng, and M. Liu, “Fuzzy IMC for Unstable Systems with Time Delay,” *2008 IEEE Pacific-Asia Work. Comput. Intell. Ind. Appl.*, vol. 2, pp. 772–778, 2008.

[14] W. F. Xie and A. B. Rad, “Fuzzy adaptive internal model control,” *IEEE Trans. Ind. Electron.*, vol. 47, no. 1, pp. 193–202, 2000.

[15] D. C. Psichogios and L. H. Ungar, “Nonlinear internal model control and model predictive control using neural networks,” in *5th IEEE International Symposium on Intelligent Control*, 1990, pp. 158–163.

[16] L. Yan, A. B. Rad, Y. K. Wong, and H. S. Chan, “Model based control using artificial neural networks,” in *the 1996 IEEE International Symposium on Intelligent Control*, 1996, pp. 283–288.

[17] A. Milias-Argeitis and M. Khammash, “Adaptive Model Predictive Control of an optogenetic system,” in *54th IEEE Conference on Decision and Control (CDC)*, 2015, pp. 1265–1270.

[18] Y. Sasaki, N. Yorino, Y. Zoka, and A. B. Rehiara, “Real-time Dynamic Economic Load Dispatch Considering Prediction Errors of PV,” in *the 20th Power Systems Computation Conference (PSCC 2018)*.

[19] Y. Zoka *et al.*, “A Study for On-demand Generation Regulation Control,” *IEEJ Trans. Power Energy*, vol. 138, no. 6, pp. 432–441, 2018.

[20] P. Kundur, *Power System Stability and Control*. USA: McGraw Hill, 1993.

[21] M. E. El-Hawary, *Electrical Power Systems*. 1983.

[22] G. Benmouyal, “The Impact of Synchronous Generators Excitation Supply on Protection and Relays,” *J. Reliab. Power*, vol. 3, no. 1, pp. 1–17, 2012.

[23] J. B. X. Devotta, “A Dynamic Model of the Synchronous Generator Excitation Control System,” *IEEE Trans. Ind. Electron.*, vol. IE-34, no. 4, pp. 429–432, 1987.

[24] A. B. Rehiara, H. Chongkai, Y. Sasaki, N. Yorino, and Y. Zoka, “An Adaptive Internal Model for Load Frequency Control Using Extreme Learning Machine,” *Telkomnika*, vol. 16, no. 6, pp. 1–6, 2018.

[25] C. He, A. B. Rehiara, Y. Sasaki, N. Yorino, and Y. Zoka, *The Application of Laguerre functions based Model Predictive Control on Load Frequency Control*. 2018.

[26] A. B. Rehiara, Y. Sasaki, N. Yorino, and Y. Zoka, “A Performance Evaluation of Load Frequency Controller using Discrete Model Predictive Controller,” in *2016 International Seminar on Intelligent Technology and Its Applications*, 2016, pp.

659–664.

[27] A. B. Rehiara, H. Chongkai, Y. Sasaki, N. Yorino, and Y. Zoka, “An adaptive IMC-MPC controller for improving LFC performance,” in *2017 IEEE Innovative Smart Grid Technologies - Asia*, 2018, pp. 1–6.

[28] M. Abdillah, H. Setiadi, A. B. Rehiara, K. Mahmoud, I. W. Farid, and A. Soeprijanto, “Optimal selection of LQR parameter using AIS for LFC in a multi-area power system,” *J. Mechatronics, Electr. Power, Veh. Technol.*, vol. 7, no. 2, p. 93, 2016.

[29] T. H. Mohamed, J. Morel, H. Bevrani, and T. Hiyama, “Model predictive based load frequency control-design concerning wind turbines,” *Int. J. Electr. Power Energy Syst.*, vol. 43, no. 1, pp. 859–867, 2012.

[30] C. He, A. B. Rehiara, Y. Sasaki, N. Yorino, and Y. Zoka, “Model Predictive Load Frequency Control using Unscented Kalman Filter,” in *IEEJ Technical Meeting on Power Engineering*, 2018.

[31] Z. Qiu, J. Sun, M. Jankovic, and M. Santillo, “Nonlinear internal model controller design for wastegate control of a turbocharged gasoline engine,” *Control Eng. Pract.*, vol. 46, pp. 105–114, 2016.

[32] C. Wong, L. Mears, and J. Ziegert, “Dead Time Compensation for a Novel Positioning System Via Predictive Controls and Virtual Intermittent Setpoints,” in *the 2009 International Manufacturing Science And Engineering Conference*, 2009, pp. 1–8.

[33] Liuping Wang, *Model Predictive Control System Design and Implementation Using MATLAB*. Springer-Verlag, London, 2009.

[34] L. Ljung, *System Identification Toolbox*. The MathWorks, Inc., 2000.

[35] J. Cao, K. Zhang, M. Luo, C. Yin, and X. Lai, “Extreme Learning Machine and Adaptive Sparse Representation for Image Classification,” *Neural Networks*, vol. 81, no. C, pp. 91–102, 2016.

[36] G. Huang, S. Song, J. N. D. Gupta, and C. Wu, “Semi-Supervised and Unsupervised Extreme Learning Machines,” *IEEE Trans. Cybern.*, vol. 44, pp. 2405–2417, 2014.

LIST OF PUBLICATIONS

A. Transactions/International Journal Papers

(1) Yoshifumi Zoka, Keita Koshimoto, Masaki Muraoka, Yasunori Kuwada, Yuki Mashima, **Adelhard Beni Rehiara**, Yutaka Sasaki, Naoto Yorino, "A Study for On-demand Generation Regulation Control," *IEEJ Trans. on Power and Energy*, Vol. 138, No. 6, pp. 432 - 441, June 2018.

(2) **Adelhard Beni Rehiara**, He Chongkai, Yutaka Sasaki, Naoto Yorino, Yoshifumi Zoka, "An Adaptive Internal Model for Load Frequency Control Using Extreme Learning Machine," TELKOMNIKA Telecommunication, Computing, Electronics and Control, Vol. 16, No. 6, pp. 791-79x, Dec. 2018 (Accepted).

B. International Conference Papers Related to This Thesis

(1) Chongkai He, **Adelhard Beni Rehiara**, Yutaka Sasaki, Naoto Yorino, Yoshifumi Zoka, "Model Predictive Load Frequency Control using Unscented Kalman Filter," *Proceedings of the IEEJ Technical Meeting on Power Engineering*, No. PE-18-206, pp.1-6, Oct. 30 - Nov.1, 2018, Jeju Island, Republic of Korea.

(2) Chongkai He, **Adelhard Beni Rehiara**, Yutaka Sasaki, Naoto Yorino, Yoshifumi Zoka, "The Application of Laguerre Functions Based Model Predictive Control on Load Frequency Control," *Proceedings of the International Conference on Electrical Engineering (ICEE2018)*, No. G3-2256, pp. 1190-1195, Jun. 24-28, 2018, Seoul, Republic of Korea.

(3) Yutaka Sasaki, Naoto Yorino, Yoshifumi Zoka, **Adelhard Rehiara Beni**, "Real-time Dynamic Economic Load Dispatch Considering Prediction Errors of PV," *Proceedings of the 20th Power Systems Computation Conference (PSCC 2018)*, PaperID. 147, pp. 1-7, Jun. 11-15, 2018, Dublin, Ireland.

(4) **Adelhard Beni Rehiara**, He Chongkai, Yutaka Sasaki, Naoto Yorino, Yoshifumi Zoka, "An Adaptive IMC-MPC Controller for Improving LFC Performance," *Proceedings of the 7th Innovative Smart Grid Technologies (ISGT Asia 2017)*, PaperNo. 287, pp. 1-6, Dec. 4-7, 2017, Auckland, New Zealand.

(5) **Adelhard Beni Rehiara**, Yutaka Sasaki, Naoto Yorino, Yoshifumi Zoka, "A Performance Evaluation of Load Frequency Controller using Discrete Model Predictive Controller," *Proceedings of the 2016 International Seminar on Intelligent Technology and Its Applications (ISITIA2016)*, PaperID. 1570279150, pp. 659-664, Jul. 28-30, 2016, Lombok Island, Indonesia.